Louisiana State University
LSU Digital Commons

LSU Master's Theses | Graduate School

2008

Freezing processes in cell suspensions evaluated using cryomicroscopy

Tathagata Acharya
Louisiana State University and Agricultural and Mechanical College, tachar1@lsu.edu

Follow this and additional works at: https://digitalcommons.lsu.edu/gradschool_theses

 Part of the Mechanical Engineering Commons

Recommended Citation
Acharya, Tathagata, "Freezing processes in cell suspensions evaluated using cryomicroscopy" (2008). *LSU Master's Theses*. 3194.
https://digitalcommons.lsu.edu/gradschool_theses/3194

This Thesis is brought to you for free and open access by the Graduate School at LSU Digital Commons. It has been accepted for inclusion in LSU Master's Theses by an authorized graduate school editor of LSU Digital Commons. For more information, please contact gradetd@lsu.edu.

FREEZING PROCESSES IN CELL SUSPENSIONS EVALUATED USING CRYOMICROSCOPY

A Thesis

Submitted to the Graduate Faculty of the
Louisiana State University and
Agricultural and Mechanical College
in partial fulfillment of the
requirements for the degree of
Master of Science in Mechanical Engineering

in

The Department of Mechanical Engineering

by
Tathagata Acharya
B.E., University of Pune, India-2004
December 2008

Acknowledgements

It gives me immense pleasure to thank all those who have made this thesis possible. First and foremost, I would like to thank my major professor, Dr. Ram V Devireddy, who has always lent his valuable time to teach and guide me. I would sincerely thank him for his technical insight and patience in motivating and mentoring me throughout this work. This work would never have been possible without him. Next, I am grateful to my committee members, Dr. Harris Wong and Dr. Todd Monroe who have been helpful and generous with their time and expertise to evaluate my thesis.

I thank all my friends and colleagues, Sreedhar, Dinesh, Ajay, Avishek and Raghava at the Bioengineering laboratory for providing me with a happy and congenial atmosphere at work, with a special note of thanks to Sreedhar who has been an exemplary senior. In addition, I would also extend my sincere gratitude to Julianne Audiffred, from the Department of Biological Engineering who provided me with cultured Jurkat and HeLa cells for my research. I could certainly not forget mentioning Chase Lambert, who had been an intern in our laboratory during summer 2007 and had helped me with my research on Pacific Oyster Embryos.

My final acknowledgement is due to my dearest parents back in India, who have always been behind me with their prayers, love and blessings. I thank my father, 'Mr. Prabir Acharya' for being the 'tower of strength' in my career and life. I thank my mother, 'Mrs. Shanta Acharya' for being the 'greatest mom' and my first teacher in any school. Hence, I would like to dedicate this work to my parents.

This work was funded by a grant from the National Institute of Health (Grant # 5R03EB005985-02). I would like to thank them for their support.

Table of Contents

List of Tables

List of Figures

Abstract

This thesis aims at evaluating the freezing response of three different cell types, Pacific Oyster embryos, Jurkats and Helas, using the technique of cryomicroscopy. The choice of cells was primarily based on supporting ongoing research work at the Bioengineering Laboratory, Department of Mechanical Engineering at Louisiana State University in Baton Rouge. On a secondary basis, the cells were chosen based on their contrasting nature. While Pacific Oyster being a favorite food in USA calls for successful techniques of cryopreservation of their embryos in order to keep up with the growing demand, Jurkat and HeLa are undesired malignant human cells that require successful cryosurgical techniques for their destruction.

The fourth chapter of the thesis addresses the freezing experiments performed on Oyster embryos at freezing rates of 5 ^{o}C/min and 10 ^{o}C/min. During these experiments, embryos were investigated for either dehydration (water transport) or intracellular ice formation (IIF). The next two chapters address the freezing experiments performed on Jurkat cells and HeLa cells respectively. Freezing rates ranging from 1 ^{o}C/min to 50 ^{o}C/min were used for these cells. Once dehydration was observed, the cells were examined for their volume shrinkage. A graph of temperature against normalized volume was plotted using the experimental results. The key cell level parameters were: Reference permeability of cell membrane to water (L_{pg}), apparent activation energy (E_{Lp}), inactive cell volume (V_b), and the ratio of surface area for water transport to the volume of intracellular water (SA/WV). The values of 'V_b' for the chosen cells were known from earlier literature. The experimental data was fit into the water transport equation, using a numerical model, in order to obtain the values of the unknown cell level parameters i.e. L_{pg} and $E_{Lp.}$ Finally, Generic Optimal Cooling Rate Equation (GOCRE) was used to determine the optimal cooling rate for the chosen variety of cells. Hence, higher freezing rates

were used on the cells, which were investigated for IIF. IIF observed using cryomicroscopy, through darkening probably supported the results for optimal freezing rates, obtained using the water transport experiments and subsequent numerical simulations.

1. Introduction

1.1 Cryobiology

Cryobiology is the branch of science that deals with the effects of freezing on living organisms and their constituent components. Cryobiology aims at restoring viable biological systems in a frozen environment for extended periods of time in order to ensure reproducibility and continuity in research and biomedical processes. One such technique of storing biological systems like cells, tissues and organs in a freezing environment to ensure their viability in future is called as cryopreservation. In contrast to cryopreservation, another important goal in the field of cryobiology is to destroy malignant tumors using low temperatures, cryosurgery.

1.2 Cryopreservation and Cryosurgery

Cryopreservation refers to the technique of storing a living organism at extremely low temperatures such as -196 ^{o}C (Mazur 1984), in suspended animation for long periods of time, so that it may be revived and restored to the same living state. Various biological systems such as cells, tissues, small multicellular organisms and even more complex organisms such as embryos could be stored using techniques of cryopreservation. Cryopreservation techniques have already been shown to be useful in a variety of mammalian systems such as red blood cells, lymphocytes, platelets, granulocytes, gametes and embryos, hepatocytes, bone marrow stem cells, cornea and skin, pancreatic tissue, heart and kidney, and have been reviewed by Mazur (1984) and McGrath et al (1975). Some of the other significant applications have been cryopreservation of human and non-human mammalian oocytes (Bernard and Fuller 1996), food freezing and tissue engineered equivalents (Oegema et al 1999), cryopreservation of parasites, insects, fish, micro-organisms and plats, including algae (Walsh 2003), cryopreservation of rat and human liver slices (Day et al 1999), fish gametes and aquatic species and spermatozoa of

various other species, including horses (Devireddy et al 2002) and human beings (Devireddy et al 1998).

Likewise, it was probably Dr. James Arnott and co-investigators; in the 1850s that first showed that cold temperatures also could be used for the treatment of malignant tumors. Ice saline solutions were directly applied to large ulcerating cancers and reduction in size, odor, discharge, pain and hemorrhage was observed. In 1961, Cooper and Lee described the first cryosurgical model (cryoprobe) (Cooper and Lee 1961). The ability of the device to produce a cryolesion in the liver was demonstrated in a cat model (Cooper 1963). Cryosurgical treatments of tumors at various organ sites such as breast, rectum, skin, brain, lung, prostrate, uterus, oral cavity, pancreas and liver have been reported elsewhere (Gage 1992, Gage and Baust 1998).

Both cryopreservation and cryosurgery require one to understand the behavior of the biological systems when a freezing stress is applied to them. Freezing is an extremely complicated phenomenon and even after decades of research, it has not been properly comprehended. Water is the chief component of all living cells and hence, it must be available for all chemical processes of life to occur. Cellular metabolism stops when all the water contained in cells is transformed into ice. It is essential to understand what happens to the cells when they are subjected to freezing temperatures. It has been seen that ice tends to form at different rates during a freezing process. When the cell in a solution is subjected to a freezing protocol, initially ice formation takes place in the extracellular space. The cell membrane acts as a barrier and prevents ice formation inside the cell. This results in supercooling of the intracellular water. The unfrozen supercooled intracellular water remains at a higher chemical potential than the partially frozen extracellular solution (Mazur 1970). This leads to a thermodynamic non equilibrium and provides the driving force for the two biophysical processes

during freezing, water transport or cellular dehydration and intracellular ice formation (Mazur 1984). Researchers have shown that while at low freezing rates water transport is the dominant mechanism, intracellular ice formation (IIF) is the dominant mechanism at very high freezing rates (Mazur 1963, Mazur 1977, Mazur 1984, Toner et al 1990). Both cellular water transport and IIF have been proved to be deleterious to the post-thaw survival of biological systems (Lovelock 1953, Mazur et al 1972). As mentioned, the freezing velocity has an enormous effect on these two biophysical processes.

When the freezing rate is too slow, intracellular water has enough time to flow out of the cell through the semi-permeable membrane and join the extracellular space. As a result, the cell loses water rapidly concentrating intracellular liquid sufficiently in order to eliminate supercooling and maintain the chemical potential of intracellular water in equilibrium with extracellular water. This results in changes in the extracellular region, such as in pH and ionic concentration and causes the tertiary structure of proteins to unfold. Hence, some of the original properties of the cell such as its biological activity are either diminished or eliminated. Such denaturation of proteins may be lethal to cell survival (Lovelock 1953). In addition, deformation of cells may also take place through mechanical interaction between extracellular ice crystals and cells (Ishiguro and Rubinsky 1994).

On the other hand, when the cell is cooled too rapidly, it doesn't have enough time to lose water in order to reach equilibrium. It thus becomes increasingly supercooled and eventually freezes intracellularly in order to attain equilibrium. Intracellular ice formation (IIF) is generally lethal as it causes injury to the intracellular structures and the cell membrane It has also been observed that the freezing rates that cause 50% IIF also correspond to only 50% cell viability. (Mazur 1963, Mazur 1977, McGrath 1985, Toner et al 1990, Toner 1993).

Thus, cooling rates that are either too slow or too fast threaten post-thaw cell viability (McGrath 1988). It has been experimentally verified for a variety of cells and it has also been shown that the curve of cell survival plotted as a function of freezing velocity has an inverse U-shape (Mazur 1977). One of the important characteristics of a cell is its permeability which shows how fast water can leave the cell at a given freezing rate. Understandably water transport through the semi permeable membrane increases as the permeability of the membrane increases at a given time and vice-versa. Hence a prescribed cooling rate being too "slow" or too "fast" is a function of cell membrane permeability to water and the probability of ice nucleation of trapped intracellular water at a given subzero temperature . The balance between the membrane's water permeability and the probability of IIF results in different optimal cooling rates for different cells. Therefore, in order to obtain an optimal freezing rate for maximum cell survival and to optimize a cryopreservation protocol, it is necessary to measure the cell membrane's permeability to water. Thus the quantitative understanding of water transport across the cell membrane at a given freezing rate is extremely necessary in order to design a cryopreservation protocol successfully. Similarly, evidence of IIF at a given freezing rate suggests that the optimal freezing rate exists below the freezing rate used.

1.3 Cryomicroscopy

Freezing response of biological systems can be studied using two different techniques called as Cryomicroscopy and Differential Scanning Calorimetry (DSC). The latter is a well established shape independent technique used in measurement of dehydration response of biological systems and has been discussed elsewhere (Devireddy et al 1998, Devireddy and Bischof 1998, Devireddy et al 1999). However, in this work only cryomicroscopy has been used to evaluate the freezing response of three different cell types. Both water transport and IIF have

been extensively studied in isolated cell suspensions using cryomicroscopy (Cosman et al 1989, Diller 1982, Toner et al 1990, Toner et al 1992). Cryomicroscopy involves application of cryogenic temperatures to cellular systems mounted under a light microscope to study the biophysical response of cells to freezing. This technique has been refined and modified over years to study the dynamic response of a variety of plant and mammalian cells under various freezing conditions. Some of the important advances in cryomicroscopy include the mounting of a cold stage on a microscope instead of cooling the entire microscope; the use of an analog control system to control the limitations of the analog control system; the use of video recordings to record the events during freezing; and the use of computer enhanced image analysis techniques to overcome the low resolution of the video recordings. The major assumption in cryomicroscopy is that the projected two dimensional area of the cell can be extrapolated to a spherical three dimensional volume. Although this assumption is reasonable for a spherical cell system, it is inappropriate for obtaining quantitative volumetric information in non spherical cell systems. Cryomicroscopy can be used to obtain images of a dehydrating cell during the course of the freezing protocol. Hence, by calculating the change in surface area from its two dimensional image and extrapolating it to its three dimensional volume one may obtain its change in volume as a function of various temperatures. Cryomicroscopy also helps in observing IIF through blackening of cells due to scattering of light by opaque ice inside cells.

1.4 Overview of Thesis

In this work, freezing responses of three different cell types (Oyster embryos, Jurkats and Helas) were evaluated using cryomicroscopy. The cells were primarily chosen to support ongoing research at the bioengineering laboratory in the department of mechanical engineering at Louisiana State University, Baton Rouge. On a secondary basis, the choice of the cells was based

on their diversity and the nature of the cell type. Need for research on Oyster embryos has been based on their great demand as food. However their availability throughout the year is limited because of their seasonal reproduction. The perennial availability of oysters probably calls for successful techniques of cryopreservation. In this work, efforts have been made in order to understand the freezing response of Oyster embryos and to identify the freezing rates at which these embryos underwent IIF. Although "fast" freezing rates at which the embryos underwent IIF could be successfully investigated, experiments based on "slow" freezing rates were limited by lack of availability of oysters. This thesis aims at providing valuable information about freezing response of Pacific Oyster embryos at two different freezing rates, for research work aimed at developing a successful cryopreservation protocol for Pacific Oyster embryos.

The second part of the thesis aims at understanding the freezing response of two different cancer cells, Jurkat and HeLa. Both Jurkat and HeLa are undesired malignant cells. Research on these cells is usually done in order to evaluate their freezing response, aiming at successful cryosurgery. In this work, these cells were investigated at various freezing rates in order to evaluate an optimal freezing rate. Efforts were also made to identify the freezing rates at which these cells underwent IIF. On a primary basis, research work on these cells was done in order to support ongoing work in Bioengineering Laboratory, Department of Mechanical Engineering, at Louisiana State University in Baton Rouge.

2. Literature Survey

2.1 Oyster

Cryopreservation in aquatic species is being studied for around 50 years (He et al 2004, Tiersch 2000). Oysters among most aquatic species have been a subject of great interest because of their great demand in the food market, which is seemingly ever growing (He et al 2004, Lin and Lung 1995, Salinas-Flores et al 2008, Salina-Flores et al 2008). Unfortunately, oysters are unavailable through most part of the year owing to their seasonal reproduction. It is believed that protocols for cryopreservation of sperm and oocytes/embryos may provide the ultimate control in selective breeding programs. Hence, efforts are being made by researchers in order to develop successful cryopreservation protocols for the storage of oyster gametes that may enable fertilization. Substantial work has been done in the field of cryopreservation of oyster spermatozoa (Dong et al 2005, Dong et al 2005, Dong et al 2006, Dong et al 2007). However, fewer researchers have worked on understanding freezing responses of oyster oocytes or embryos with some of the notable work being mentioned in this section.

Salinas-Flores et al in 2008, worked on the determination of membrane permeability characteristics of Pacific Oyster oocytes and development of optimized methods to add and remove ethylene glycol. In this work, it was determined that the oocytes behaved as ideal osmometers with an inactive cell volume of 0.48. These oocytes were exposed to sodium chloride solutions of 0.6 to 2.3 osmoles, when they fertilized at rates equivalent to oocytes in sea water. Volume changes of 27.3% and 38.1 +/- 1.2% were observed at the two concentrations respectively. Finally, these findings led to considerable reduction in handling when it was seen that post-thaw fertilization did not differ significantly between the earlier published step addition method and the now used single step addition method.

In a separate work, Salinas-Flores et al in 2008 estimated the survival of Pacific Oyster oocytes in relation to IIF. The effect of IIF in oyster oocytes was studied using cryomicroscopy and transmission electron microscopy (TEM). At each step of the protocol, viability of oocytes was assessed through an initial experiment. Although no evidence of IIF in the oocytes was reported through cryomicroscopy, it was revealed by TEM that the oocytes underwent IIF. Two major viability losses were reported which were at -35 ^{o}C and when the oocytes were plunged into liquid nitrogen.

Tervit et al in 2005 attempted to develop a successful cryopreservation protocol for Pacific Oyster oocytes. Ethylene Glycol (10%) and Dimethyl Sulfoxide (15%) were reported as most effective cryoprotectants resulting in high post-thaw fertilization rates of 51 +/- 8 % and 45.1 +/- 8.3% respectively. Propylene Glycol was reported as less effective and Methanol was reported as not effective in post-thaw fertilization. It was also said that the use of Milli-Q water instead of sea water as a base medium, and a 5 minute isothermal hold at -10 ^{o}C or -12 ^{o}C significantly improved fertilization. The optimal cooling rate post-thaw was evaluated to be 0.3 ^{o}C/min. The post-thaw fertilization rates from oocytes were reported to be within the range of 0.8 to 74.5 %.

Lin et al in 1999 studied the factors affecting survival of cryopreserved oyster embryos. A conventional two step freezing procedure was developed and optimized in order to cryopreserve oyster embryos. The effects of cooling rate, choice of cryoprotectant, and seeding temperature on the survival of oyster embryos were studied. Using the optimized factors, improved survival rates of 78 +/- 8% and 83 +/- 7% were reported using 2 M Me(2)SO and Glycerol respectively. The survival of oyster embryos after freezing was reported over a broad range of cooling rates between 0.5 and 16 ^{o}C/min.

Gwo in 1995 examined the critical variables that were associated with oyster cryopreservation. The critical variables as listed by him were embryo developmental stage, type and the concentration of cryoprotectant, equilibration time and the freezing rate. In his experiments, percentage survival was evaluated from the number of recovered embryos that swam actively 12 hours after thawing.

As mentioned before, in this work, attention was paid to Pacific Oyster embryos and how they behaved when subjected to freezing. The embryos were primarily investigated for evidences of IIF at two different freezing rates.

2.2 Jurkat

Jurkat cells are most commonly used to study acute T cell leukemia, a rare blood and bone marrow cancer (Barmak et al 2003). Although substantial research work has been done in the field of cryobiology of prostate tumor cells (Wolkers et al 2007), breast cancer cells (Hong and Rubinsky 1994), and uterine fibroid tumor tissue cells (Devireddy et al 2001), Jurkats cells have been relatively less understood. There is an increasing need to understand the low temperature behavior of Jurkat cells not only for immunological reasons but also for the application in adoptive tumor therapy (Barmak et al 2003). Two other reasons for choosing Jurkat cells in the present work were because of their robustness and easy availability and finally, to support ongoing research in the laboratory.

Thirumala et al in 2007 studied freezing and post-thaw apoptotic behavior of cells in the presence of palmitoyl nanogold particles. The main aim of their work was to evaluate the freezing response of both Jurkat and HeLa cells in presence of commercially available nanoparticles. The cells were incubated with nanoparticles and Differential Scanning Calorimetry (DSC) technique was used to generate the volumetric shrinkage response during

freezing at 20 ^{o}C/min. The cells were also investigated in presence of a commonly used cryoprotectant, 10% dimethyl sulfoxide (DMSO). A model of water transport was fit to the experimentally obtained volumetric shrinkage data in order to calculate the reference permeability of cell membrane (L_{pg}) and the activation energy (E_{Lp}). For Jurkat cells, the reference permeability of cell membrane (L_{pg}) was found to be within the range of 0.05 to 0.16 μm/min-atm, while the range of activation energy (E_{Lp}) was between 9.5 kCal/mol and 35.9 kCal/mol. Generic Optimal Cooling Rate Equation (GOCRE) was used to predict the optimal freezing rate of Jurkat cells in presence and absence of nanoparticles and DMSO. Jurkat cells were frozen at three different rates using a commercially available control rate freezer in presence and absence of DMSO and nanoparticles in order to investigate their post thaw viability and apoptotic (programmed cell death) response. However, the Jurkat cells being treated in this manner showed an increase in their adhesive property and adhered strongly to the bottom of the culture plate. This prevented any further analysis on these cells in their work.

2.3 HeLa

HeLa cell like Jurkat is also an immortal cell line derived from cervical cancer cells of one Mrs. Henrietta Lacks (Rebecca 2001), who died from her cancer on October 4, 1951. Similar to Jurkat cells, these cells were also chosen for analysis because of their robustness, easy availability, and because they are relatively less understood among all cancer cells. In addition, analysis of these cells was also aimed at supporting previous and ongoing research in the laboratory.

Thirumala et al in 2007 also evaluated the freezing response of HeLa cells in presence and absence of nanoparticles and 10% DMSO. For HeLa cells, reference permeability of cell membrane (L_{pg}) was reported to be in the range between 0.08 and 0.23 μm/min-atm, while their

activation energy (E_{Lp}) ranged from 10.9 to 37.4 kCal/mol. In a similar way GOCRE was used to predict the optimal freezing rate of HeLa cells in presence and absence of nanoparticles and 10% DMSO. Similar to Jurkat cells, the post-thaw viability of HeLa cells was investigated by cooling these cells at three rates in the presence and absence of nanoparticles and DMSO. No significant effect of nanoparticles or DMSO alone was reported on HeLa cell viability prior to freezing. However, the post-thaw results from HeLa cells showed that the nanoparticles increased the measured post-thaw apoptotic response when cooled at 1 ^{o}C/min, which probably suggested the possible therapeutic use of nanoparticles in cryodestructive procedures.

To the best of our knowledge, not much work has been done in the field of analysis of freezing response of Jurkat and HeLa cells which involves measurement of membrane permeability characteristics and prediction of optimal freezing rate. The work in this thesis sought to evaluate these characteristics using the standard technique of cryomicroscopy in order to aid previous work done by Thirumala et al. using the technique of differential scanning calorimetry.

3. Materials and Methods

3.1 Methods of Evaluation of Freezing Response of Cells

3.1.1 Water Transport Model

A mathematical model governing this physical phenomenon was derived by Mazur in 1963. It was subsequently treated by Levin et al. in 1979, Schwartz and Diller in 1983 and Shabana and McGrath in 1988.

Some of the important assumptions used in deriving the water transport model are:

- The cells undergoing dehydration were idealized biological cells which meant that they were assumed to be open thermodynamic systems having semi permeable boundaries.
- The protoplasm was assumed to be an ideal dilute solution and hence Raoult's law of partial pressure was valid for it.
- The cells were assumed to have infinite extracellular space. Cellular space was the volume of geometry being studied.
- The surface areas of the cells were assumed to be constant.
- The temperature differential across the cell membrane was considered as negligible.
- The concentration gradient was only assumed between the extracellular solution and the intracellular cytosol.
- There was no pressure gradient across the cell membrane (Mazur 1963).

If the protoplasm is assumed to be an ideal dilute solution, Raoult's law will apply:

$$p_i = p^o x^i \quad \ldots. (1)$$

In equation (1) p_i, p^o and x^i are the vapor pressure of intracellular water, vapor pressure of pure water and mole fraction of intracellular water respectively.

Hence, taking logarithms on both sides and differentiating with respect to temperature, we obtain

$$\frac{d(\ln p_i)}{dT} = \frac{d(\ln p^o + \ln x_i)}{dT} \ldots . (2)$$

According to Clausius Clapeyron equation, one may write:

$$\frac{d(\ln p^o)}{dT} = \frac{L_v}{RT^2} \ldots . (3)$$

where L_v is the molar heat of vaporization. Therefore, using equations (2) and (3):

$$\frac{d(\ln p_i)}{dT} = \frac{L_v}{RT^2} + \frac{d(\ln x_i)}{dT} \ldots . (4)$$

Considering the change in vapor pressure of the external medium with temperature, and using Clausius Clapeyron equation, one may write:

$$\frac{d(\ln p_e)}{dT} = \frac{L_s}{RT^2} \ldots . (5)$$

where L_s is the molar heat of sublimation and p_e is the vapor pressure of the external medium. Even if solutes are present in the external medium, some liquid solution will be present at temperatures above the eutectic point. Any such solution has been assumed to be in equilibrium with ice and hence will have a vapor pressure, p_e.

However, it is known that $L_s - L_v = L_f$…..(6) (Molar heat of fusion)

Subtracting equation (4) from equation (5), one may arrive at:

$$\frac{d(\ln \frac{p_e}{p_i})}{dT} = \frac{(L_f)}{RT^2} - \frac{d(\ln x_i)}{dT} \ldots . (7)$$

Integrating equation (7) with respect to temperature T, between the freezing temperature of water and a given subzero temperature leads to the following:

$$-\ln\frac{p_e}{p_i} = -\frac{L_f}{R}\left(\frac{-1}{T}+\frac{1}{T_f}\right) + \ln\frac{V-V_b}{(V-V_b)+n_2v_1} \ldots . (8)$$

where T_f is the equilibrium freezing temperature of water, n_2 is the number of moles of the solute, v_1 is the molar volume of water, and V_b is the inactive cell volume that does not participate in osmosis.

Water transport from the cell is measured as a function of the change in volume of the cell with respect to temperature. Davson and Danielli in 1952 showed that the rate of loss of water from a cell is given by:

$$\frac{dV}{dt} = L_pA(\Pi_i - \Pi_e) \ldots . (9)$$

Where t is time in minutes, L_p is the permeability constant (μ^3 of water per μ^2 of surface of cell membrane per min. per atmosphere difference in osmotic pressure between inside and outside the cell), A is the cell membrane area and Π_i and Π_e are the internal and external osmotic pressures.

However, Π being a function of vapor pressure is given by:

$$\Pi v_1 = RT\ln\frac{p_o}{p} \ldots . (10)$$

where p_o and p are the vapor pressures of pure water and water in solution. Using equations (9) and (10), one may arrive at:

$$\frac{dV}{dt} = \frac{L_pART}{v_1}\ln\frac{p_e}{p_i} \ldots . (11)$$

However, it is the rate of cooling that one may be interested in and the simplest equation for the rate of cooling is given by:

$$\frac{dT}{dt} = B \ldots . (12)$$

where T is temperature and B is the freezing rate. Thus using equations (8), (11) and (12), we arrive at the following differential equation which was earlier derived by Mazur in 1963:

$$\frac{dV}{dT} = -\frac{L_P A\, R\, T}{v_w B}\left[\ln\frac{(V - V_b)}{(V - V_b) + v_w(n_s)} - \frac{\Delta H_f}{R}\left(\frac{1}{T_R} - \frac{1}{T}\right)\right] \ldots (13)$$

Levin and co workers in 1976 showed that the temperature dependence of membrane permeability to water (L_p) was expressed as an Arrhenius relationship (Levin et al 1976), which would lead to:

$$L_P = L_{Pg} \exp\left[\frac{E_{Lp}}{R}\left(\frac{1}{T} - \frac{1}{T_R}\right)\right] \ldots (14)$$

L_{pg} = Reference permeability of cell membrane

E_{Lp} = Activation energy for permeation

V_b = Inactive cell volume

A = Surface area of the cell membrane = $A_o[V/V_o]^{2/3}$

v_w = Partial molar volume of water

B = Cooling rate

T_R = Equilibrium freezing constant for pure water

$\Delta H_f = L_f$ = Latent heat of fusion

n_s = Number of moles of salt

T = Absolute temperature

3.1.1.1 Optimal Cooling Rate

The plot of cooling velocity with the viability of the cells looks like the following.

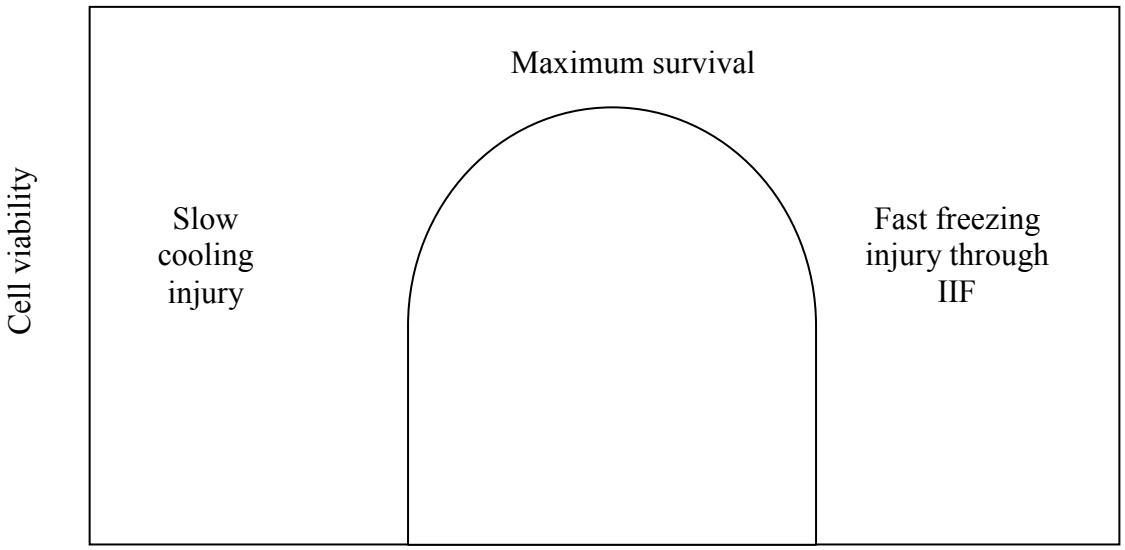

Figure 3.1: The Inverse 'U' Curve

It can be seen that the optimal cooling rate is somewhere between fast and slow cooling rates. Optimal cooling rate for a given biological system corresponds to its maximum survival or viability. Figure 3.1 shows a representative survival curve for a cell type as a function of cooling rate. As shown, the fraction of survival progressively increases with increasing cooling rate as the harmful effects of water transport reduce. Survival reaches a maximum which presumably just precedes the first appearance of IIF. Following this, as IIF increases, viability falls. This leads to the investigation of precise quantitative information about the rate and amount of water transport out of the cells at subzero temperatures. It has been shown that for a given cell type, the cooling rate depends on various cell level parameters including L_{pg}, E_{Lp}, V_b, and V_o (the cell volume) and the available cell membrane surface area, SA. The three parameters V_b, V_o, and SA

can be collapsed into a single parameter, SA/WV where WV is the initial intracellular water volume. Hence $WV = V_o - V_b$.

Since different cells have different biophysical parameters, the optimal cooling rate depends on the cell type. There is a huge diversity in the values of optimal cooling rate ranging from ~1 ^oC/min (bone marrow cells) to ~ 1000 ^oC/min (red blood cells) (Mazur 1970, Mazur et al 1972). Following Mazur, and others (Devireddy et al 1998, Devireddy et al 2000, Devireddy et al 2002), Thirumala and Devireddy in 2005, defined the optimal cooling rate as the highest cooling rate that taps 5% of the initial intracellular water (WV) at an end temperature of -15 ^oC. The water transport equation (equations 13 and 14) was numerically solved by them using a fourth order Runge-Kutta method to calculate the values of optimal cooling rate over a wide range of cell level parameters, reference permeability of cell membrane (L_{pg}), apparent activation energy (E_{Lp}), inactive cell volume (V_b), diameter (D), end temperature (T_{end}), and the ratio of surface area to volume of intracellular water (SA/WV). After learning about the variation of the predicted optimal cooling rate (B_{opt}) with the above mentioned parameters through various plots, a Generic Optimal Cooling Rate Chart (GOCRC) was prepared by them which provided information about variation of B_{opt} (on Y-axis) with E_{Lp} (on X-axis) at SA/WV =1.0 and L_{pg} = 1.0 μm/min-atm. There was an exact linear relationship between $L_{pg,}$ SA/WV and B_{opt} values which related the cooling rate values on Y-axis (B_{GOCRC}) to optimal cooling rate for any given arbitrary biological system.

$$B_{opt} = B_{GOCRC} * (L_{pg})_a * (\frac{SA}{WV})_a \dots\dots (15)$$

$(Lpg)_a$, and $(SA/WV)_a$ were the actual cell level parameters of the biological systems for which B_{opt} was to be calculated. The above equation was further simplified and the following

equation called as the Generic Optimal Cooling Rate Equation was obtained, the details of which could be found elsewhere (Thirumala and Devireddy 2005).

$$B_{opt} = 1009.5 * \exp^{(-0.0546 * E_{Lp})} * \left(L_{pg}\right) * \frac{SA}{WV} \ldots\ldots (16)$$

B_{opt} = Optimal cooling rate

E_{Lp} = Activation energy for the permeation through cell membrane

L_{pg} = Reference permeability of cell membrane

SA = Surface area of cell membrane

WV = Volume of water contained inside the cell membrane

Hence, the **optimal cooling rate** is an important parameter that improves the post thaw viability of cells. The existence of an 'optimal cooling rate' for different varieties of cells has been proved before with some of the major work being done in studying mouse marrow stem cells, yeast, and human red cell (McGrath et al 1975, Meyer et al 1975, Nag and Street 1973, Raccach et al 1975, Simon 1972, Thorpe et al 1976).

Looking at the curve of optimal cooling rate, it is evident that one might be able to calculate the value of optimal cooling rate if he has all the information about the membrane permeability characteristics (L_{pg} and E_{Lp}), and the cell level parameters (SA/WV) during slow freezing. Slow freezing events take place on the left hand side of the inverse U curve.

However, one might also obtain similar information from the right hand side of the curve which is associated with fast freezing. As mentioned before, the right hand side of the inverse-U curve shows freezing rates at which a given cell type undergoes intracellular ice formation (IIF). The following equations although not used in the present work are useful tools for understanding

cellular behavior under high freezing rates. The main aim of using these equations is to predict the occurrence of percentage intracellular ice formation (PIIF) at a given freezing rate.

3.1.2 IIF Model

$$I_{het}^{SCN} = \Omega_o \frac{N^S}{N_0^S} \frac{\eta_0}{\eta} \left[\frac{T}{T_{f0}}\right]^{\frac{1}{2}} \exp\left[\frac{-\kappa_0 (\frac{T_f}{T_{f0}})^4}{\Delta T^2 T^3}\right] \dots (17)$$

Temperature and the concentration dependency of viscosity which was given by:

$$\eta = \eta_w(T) \exp\left[\frac{2.5\Phi_m}{1 - Q\Phi_m}\right] = A\left[\frac{T}{225} - 1\right]^{-\mu} \exp\left[\frac{2.5\Phi_m}{1 - Q\Phi_m}\right] \dots (18)$$

The symbols used in the above equations have the following interpretations:

I_{het}^{SCN}= Heterogeneous nucleation rate through surface controlled nucleation

Ω_o = Kinetic parameter under isotonic conditions

κ_0 = Thermodynamic parameter under isotonic conditions

N^S = Number of water molecules in contact with the substrate

N_0^S = Number of water molecules in contact under isotonic conditions

η = Viscosity of cytoplasm

η_0 = Viscosity of cytoplasm under isotonic conditions

T_f = Equilibrium freezing temperature

T_{f0} = Equilibrium freezing temperature under isotonic conditions

ΔT = Degree of super cooling below the freezing point

η = Viscosity of pure water

Φ_m = Volume fraction of solutes (salts+proteins)

Q = Interaction parameter = 0.609375

A = 0.139 cP for water

μ = -1.64

T = Absolute temperature

The chief assumption in the IIF model is that the crystallization time inside a cell is negligible when compared to the nucleation time. In other words, ice formation is a statistical phenomenon and phase change takes place throughout the liquid surface immediately (Toner et al 1990).

Reiterating the above using mathematical equations, one could write:

Since:

$$I^s = \frac{1}{V_w N}\frac{\partial i^*}{\partial t} \ldots (19)$$

Where:

I^s = Heterogeneous nucleation rate

N = Number of unfrozen cells at time t

V_w = Volume of water in the cell

$$\frac{\partial i^*}{\partial t} = \text{Frequency of critical cluster formation}$$

$$\frac{\partial i^*}{\partial t} = -\frac{\partial N}{\partial t} \ldots . (20)$$

From equations (19) and (20) we have:

$$I^s = \frac{1}{V_w N}\frac{-\partial N}{\partial t}$$

$$I^s(V_w, T)V_w(T)\,\partial t = -\frac{\partial N}{N}$$

$$I^s(V_w, T)V_w(T)\frac{\partial t}{\partial T}\,\partial T = -\frac{\partial N}{N} \ldots . (21)$$

Since the freezing rate is given by:

$$B = \frac{\partial T}{\partial t} \ldots . (22)$$

Using equations (21) and (22), one could arrive at the following:

$$\int_{T_f}^{T} \frac{I^s(V_w, T)V_w(T)\ \partial T}{B} = \int_{N}^{T} -\frac{\partial N}{N} \ldots (23)$$

Where T = total number of cells used in the freezing experiment

and $1 - \frac{N}{T} = \text{PIF (percentage intracellular ice formation)}$

Probability of intracellular ice formation through surface controlled nucleation (SCN) could hence be found by replacing volume (V) by area (A) in equation (23), and hence integrating between the seeding temperature and a given subzero temperature, which is as follows (Toner et al 1990, Toner 1993).

$$PIF^{SCN} = 1 - \exp\left[\frac{-1}{B}\int_{Tseed}^{T} AI^{SCN}\ dT\right] \ldots (24)$$

$$PIF^{VCN} = 1 - \exp\left[\frac{-1}{B}\int_{Tseed}^{T} VI^{VCN}\ dT\right] \ldots (25)$$

The total probability could be calculated as the superposition of both modes of IIF, i.e. SCN and VCN and hence could be written as:

$$PIF = PIF^{SCN} + (1-PIF^{SCN})PIF^{VCN} \ldots (26)$$

3.2 Introduction to Cryomicroscopy

The only technique used in this work was cryomicroscopy, which as mentioned earlier involved application of cryogenic temperatures to cellular systems mounted under a light microscope in order to study the biophysical responses of cells.

The first known practical light microscope was invented and applied by Van Leeuwenhoek and Hooke for laboratory studies of micro-organisms during 1660s (Anderson 1965). The first use of cryomicroscopy probably dates back to somewhere during middle 1800s, when Julius Sachs, one of the pioneers of cryobiological research merged microscopy and low temperature biology (Pringsheim 1932). Being a founder of plant physiology, he was interested to learn how plant tissues were injured under the influence of environmental stressors like freezing and hypertonicity. Following his master's footsteps, Herman Müller-Thurgau, a noteworthy PhD student of Sachs, conducted microscope experiments to study cellular response to freezing stress and the significance of super cooling (Müller-Thurgau 1880).

Perhaps, one of the most notable contributions in the field of cryomicroscopy was from Professor Hans Molisch, PhD. He built the first known cryomicroscope, a double walled cubical wooden box which was 27 cm high, 33 cm long and 33 cm broad. The space between the walls was 7 cm wide and was filled with saw-dust with an intention to surround the inner cavity with a poor heat conductor. The inner cavity of the box was made up of zinc plate and held an insert which also was made up of zinc plate and was intended to hold the microscope. There was one column to support this insert. In addition, there was a light duct which was also made from zinc

plate and to an extent by metal tubes. Following is an isometric view of Prof Molisch's apparatus redrawn from his publication (Molisch 1982).

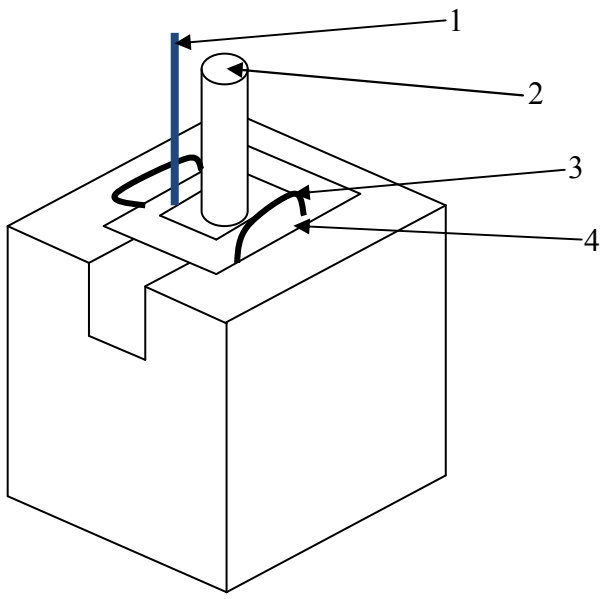

Figure 3.2: Professor Molisch's microscope (Molisch 1982)

1 = thermometer

2 = eye piece of the microscope

3 = handles to remove the top

4 = inner cavity of the box

In the above set up the inner cavity of the box contained the microscope and the inner wall of the box served as the receptacle for the freezing mixture. The compartments for the microscope and the freezing mixture were closed by a lid which had apertures for fine adjustments of the microscope. As shown in the above diagram, a sensitive thermometer was used whose bulb was almost in contact with the lid to be frozen. It was desirable to let the

apparatus and the microscope get cold in an unheated room before actual work started. Later, the ice compartment was filled completely with a freezing mixture. Generally, the freezing mixture would be a mixture of ice and sodium chloride. The microscope with the slide in place was put in the box, and the apparatus was closed with the lid. Major operations such as focusing, adjusting the mirror, and moving the slide were easily accomplished by means of the earlier described fittings.

Several decades later, during 1960s, Diller and Cravalho (Diller 2005) used the closed loop feedback control system capable of pre-programming and independent regulation of the specimen cooling rate and instantaneous temperature. The design of the system incorporated a small thermal mass in conjunction with an analog electronic circuit to facilitate a rapid response time constant. The specimen was cooled by a convective circulation of a stream of cold dry nitrogen gas directly below a thin glass plate on which the cell specimen was mounted. Heating was done through application of electrical voltage across a transparent thick film coat applied to the bottom side of the plate. Cooling load applied was approximately steady state. However, heating could be modulated extremely quickly in accordance with variations in electrical voltage input from controller. Specimen temperature was monitored continuously by a micro-thermocouple positioned directly in cell suspension. In this system, simple proportional control logic was applied via the hardwired circuitry of the analog system to the thermocouple input signal in comparison with a pre-programmed electrical representation of the desired specimen thermal history. Simultaneous cooling and heating of the sample specimen could be adjusted to allow thermal transients to 7000 ^{o}C/min. This enabled a comprehensive study of the ice nucleation and cooling conditions necessary for intracellular ice formation (IIF) in human erythrocytes (Diller and Cravalho 1970, Diller 2005).

3.2 The Experimental Setup

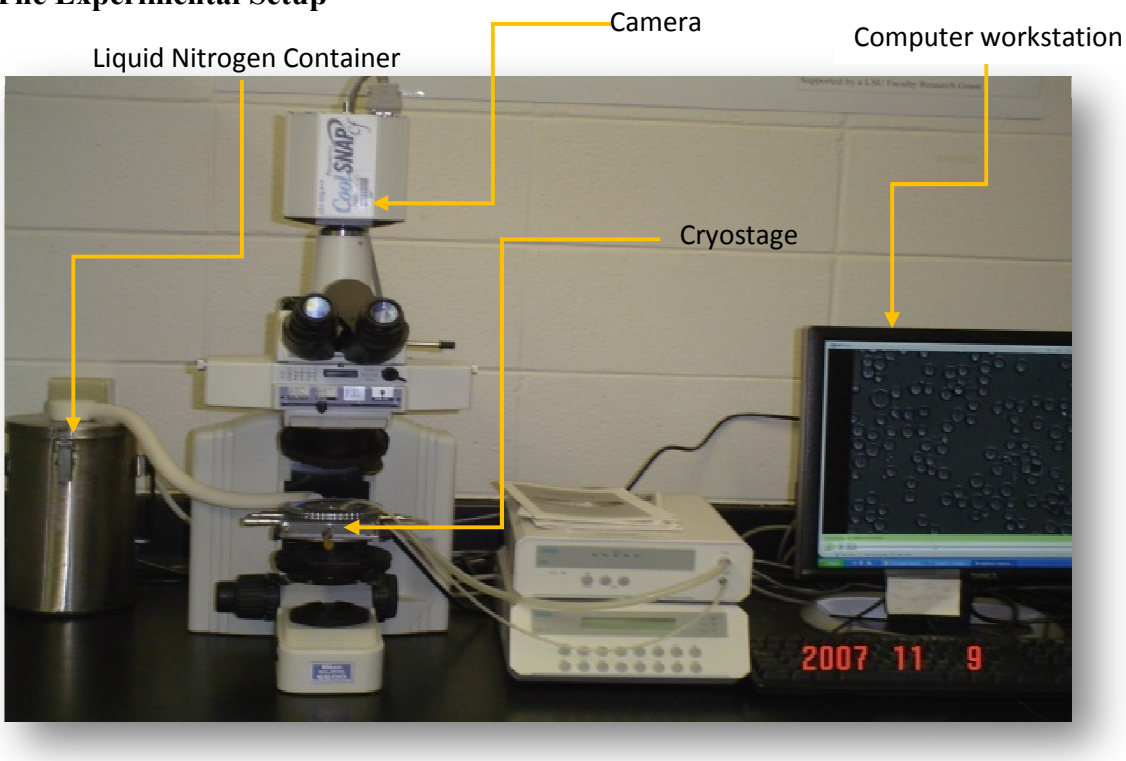

Figure 3.3: Cryomicroscopy combines the functions of temperature control, image storage and event control, and image analysis through the components shown above.

The cryomicroscopy system integrated the functions of sample temperature control, image storage and event correlation, and image analysis. Some of the other developments include a flexible commentary of recorded experiments through the electronic combination of the computer generated graphics with microscope video images; and integration of system functions under software control. Hence, the present applications of the enhanced cryomicroscopy system basically included the volumetric response of cells to osmotic perturbations and the study of the dependence of intracellular ice formation on temperature and cooling rate (Cosman et al 1989). While volumetric response would help in analysis of water transport, intracellular ice formation could be shown by darkening under microscope. Following were the basic functions of the cryomicroscope and the description of the components useful for their execution.

3.3.1 Temperature Control

Temperature control was one of the most important functions of a cryomicroscope. It was an essential function that was required to understand the freezing response of a cell at a particular temperature. The initiation of sample freezing was considered as a part of this function. Thermal history of the sample was programmed, executed and hence recorded. Following were the components of the cryomicroscopy system that executed this function.

3.3.1.1 Cryostage

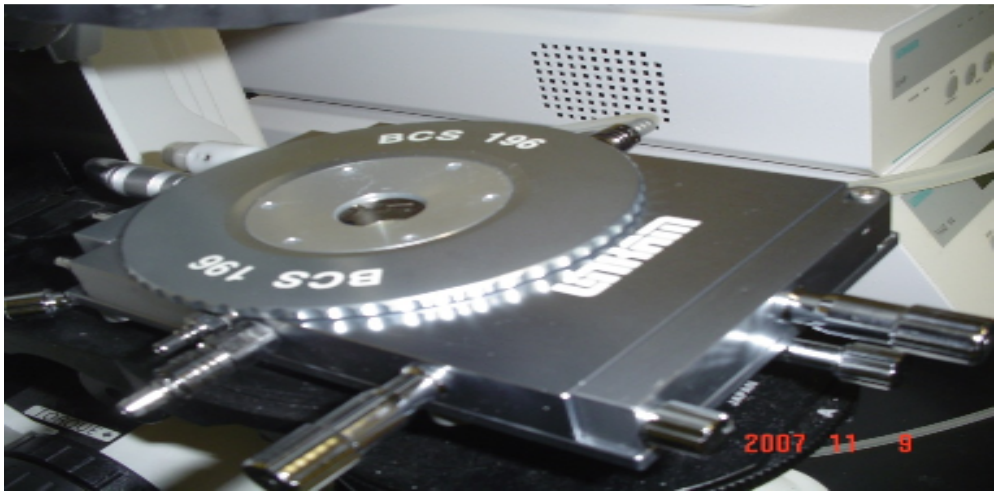

Figure 3.4: Above picture shows the cryostage used for present work. All freezing experiments took place inside the cryostage which was capable of controlled cooling and heating between -125 ^{o}C and 160 ^{o}C at rates between 0.01 ^{o}C/min and 130 ^{o}C/min.

The cryostage was the metallic box within which the freezing experiments took place. Gaseous nitrogen, cooled by passage through a coil immersed in liquid nitrogen was used as the refrigerant for the cryostage. The cryostage used was manufactured by LINKAM Scientific (Surrey, United Kingdom; Model BCS 196) and was capable of controlled cooling or heating between -125 ^{o}C and 160 ^{o}C at rates between 0.01 ^{o}C and 130 ^{o}C /min. Sample temperature was measured by a platinum resistance thermocouple at a point on the heated cryostage window. The

temperature controller provided the window heater with the power needed to counterbalance the refrigerant and hence maintain the sample at the desired temperature or setpoint. A time varying setpoint was created by the computer when running temperature control software. The cryostage was mounted with a circular quartz crucible to hold the cell suspension during freezing.

3.3.1.2 Temperature Control Software

Linksys 32 was a temperature control and data capture software system. The freezing process inside the cryostage could be controlled either manually using the function keys on an instrument called TMS 94 or using the Linksys 32 software. While using Linksys 32, if the temperature-control status display showed the message 'NO COMM Programmer not connected,' it meant that the software did not recognize that there was a temperature programmer connected. It meant that the user needed to click on the file menu-bar and select the 'connect 'option. The software would now tell the user to power on the equipment connected to the selected command port. After clicking 'OK', the user should click on 'setup' option on the menu-bar and select 'temperature controller.' At this, the 'Linksys 32 Setup' window would appear and the user would be prompted to click on the command port at which the cable would have been connected.

After closing this window, the software would ask the user to 'Power on' the LINKAM equipment connected to command port 1. Following this, the user might notice live temperature appearing on display. This would suggest that the software was ready to accept inputs control. Linksys 32 could setup complex temperature profiles up to 100 ramps. Rate, limit and hold time could be individually programmed for each ramp. To start with, Linksys 32 needed to be instructed to use 'Temperature Profile' instead of manual control although the user could overwrite the temperature profile with manual control at any point of time.

The temperature profile table contained a profile with 6 ramps. At the end of the hold time of each ramp, the programmer would move to the next ramp and so on until the profile was complete. For example, in ramp 1 the temperature programmer would first cool the stage to 4 ^{o}C at a rate of 10 ^{o}C/min and then would hold for a minute before moving onto the next ramp. The stage would then be cooled at a slower rate of 1 ^{o}C/min to -5 ^{o}C. If there was no holding time set, the stage would start cooling immediately after reaching the temperature of 4 ^{o}C. In order to enter the values in the table, the user could simply type the values desired. However, in order to help the software register the value, the user either needed to press enter or click on the next box after entering the value. Finally, the user needed to press 'start' in the temperature profile toolbar to start heating/cooling run. The active ramp of the profile was shown in light blue color. The values in the profile could be changed at any time during the run and could also over ride the profile with the manual temperature controls. It was also possible to save a temperature profile to enable quick setup of similar experiments. Hence summarizing, Linksys 32 was extremely useful software that enabled the user to accurately program the freezing protocol for a given variety of biological system, and execute the steps within the protocol. The software could help carry out various steps like freezing, holding at a temperature for a given period of time and thawing without much manual intervention. The software also had certain capabilities such as memorizing an often used protocol even after the system had been switched off.

3.3.2 Image Control and Event Correlation

In the field of cryomicroscopy, cells are being observed and their reactions to a thermal change are analyzed. The microscopic images must be recorded so that subsequent detailed observation and analysis might be performed. Events occurring during a temperature excursion must be annotated with the corresponding time and temperature from the beginning excursion.

For storing images, usually video cameras and recorders are preferred methods. Some of the major utilities that they provide are ability to capture dynamic processes through rapid image update (25-30 pictures/second), inexpensive and reusable recording medium, and allowing quick inspection due to rapid image capturing and not requiring further processing. The cryomicroscope system was fitted with a Newvicon camera (Hamamatsu, Photonics, Bridgewater, NJ) to snap images of the cells responding to a given freezing stress. Multiple images were transferred through a data cable to a DELL workstation. Commercially available software called 'Metacam' was used to stack the images of the cellular system undergoing freezing. Movies were made by linking the images in the stack which provided information about the response of cells to an applied freezing stress. Metacam also provided the user freedom to delete undesired images, slow down or to increase the speed of the movie.

3.3.2.1 Optical Information

It was extremely important to have the microscope set up correctly, especially when working at high magnifications or when looking at difficult objects such as cells in suspensions. Following were some precautions that were taken to set up the most important features of the microscope such as the light source and condenser lens. The adjustment of the light source was necessary only when the microscope was first installed or when the bulb was replaced, provided that the adjustments were not disturbed. In order to correctly view the activity underneath the microscope, light needed to pass through the cellular suspension placed on a transparent petri-dish on the crucible of the stage. The two significant biophysical phenomena namely 'Water Transport' and IIF could be seen through the effect of light rays passing through the cellular suspension in the petridish. Following is a simple line drawing showing the essential parts of the microscope's optical path.

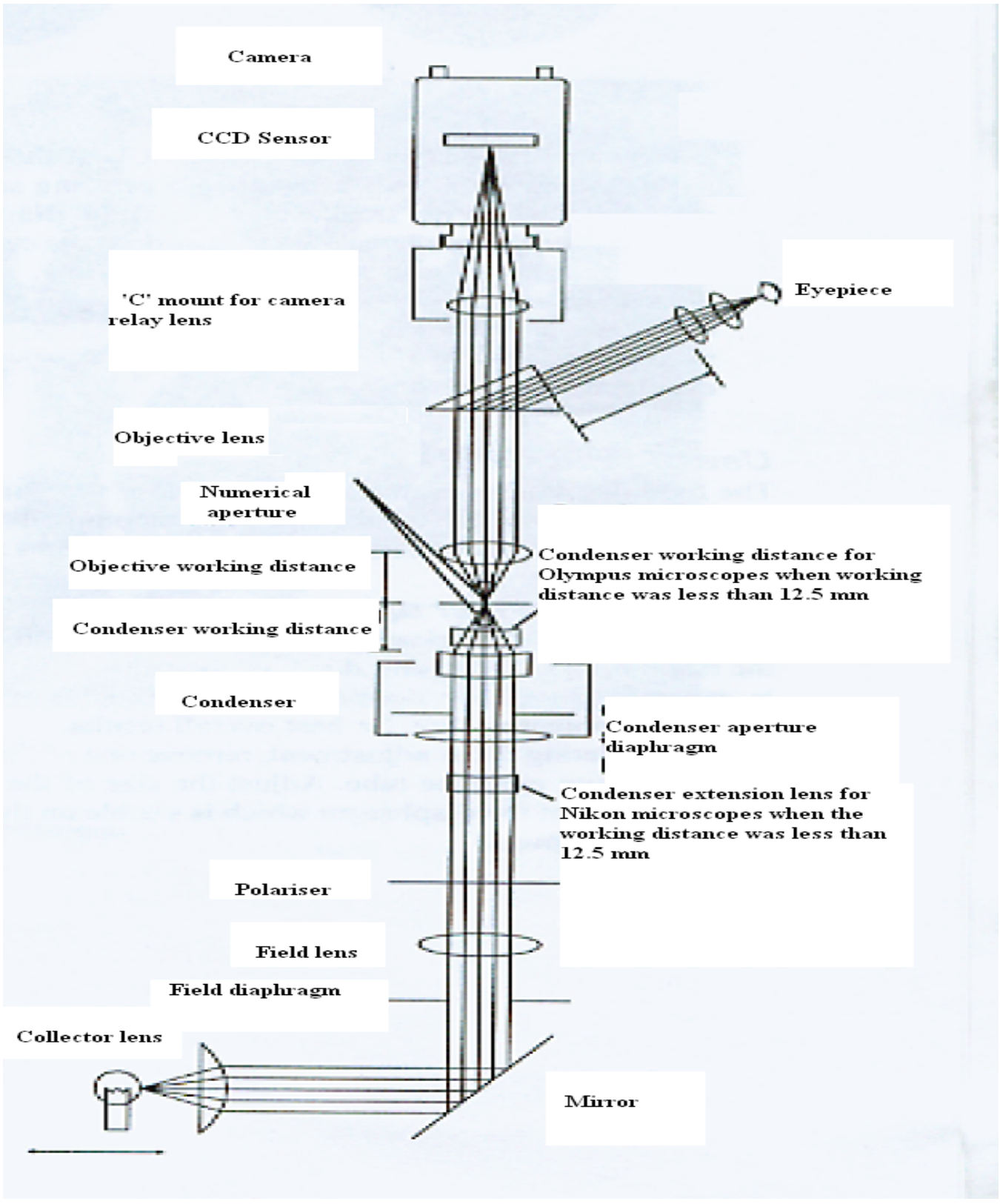

Figure 3.5: Line diagram of optical cryomicroscope (Linkam Scientific Instruments Ltd)

Following precautions needed to be taken before starting the experiments:

1. The field diaphragm on the base of the microscope was opened to its largest extent and a flat, thin piece of paper was placed over it.
2. The light source was turned to its maximum output.
3. The lamp housing was slid backwards and forwards until the image of the bulb filament was visible on the paper.
4. The lamp vertical centering ring and the lateral centering screw on the lamp housing were adjusted to center the filament.
5. The lamp housing was pulled slightly forward until the filament image was diffused, or alternatively a diffusing filter was fitted.

3.3.2.2 Centering the Condenser Lens

It was very important to have a focused, centered and condensed light beam at all times to ensure the correctness in the setting of the field diaphragm and condenser.

The field diaphragm controlled the diameter of the illuminated area on the specimen surface in relation to the field of view of the microscope. By stopping down the field diaphragm, until it was slightly larger than the field of view, it could reduce stray light, which in turn increased image definition and contrast.

Using the condenser aperture diaphragm, the numerical aperture of the illuminating system of the microscope could be adjusted and the resolution, contrast and the depth of focus could be determined. It was generally stopped down to 70-80% of the numerical aperture of the objective lens for the best overall result. After completing the focus adjustment, one of the eyepieces was removed and the empty eyepiece tube was looked into. The size of the diaphragm

was adjusted, observing the image of the diaphragm that was visible on the bright circle of the objective exit pupil (Linkam Scientific Instruments Ltd).

3.3.3 Image Analysis

Image analysis could be defined as the extraction of quantitative data from the recorded images of a cryomicroscope experiment in a form which could be utilized by data reduction algorithms. Some of the important methods of image analysis have been mentioned below (Cosman et al 1989):

a. Mechanical planimetry of still photos: Using this method, the cross sectional area of the cell could be evaluated, which might be useful in approximating the cell volume. This method required rapid photography to capture dynamic images. Paper tracings of the video images might also be considered as mechanical planimetry.
b. Electronic methods of area analysis: This method involved the computation of cell area within a computer generated circle. The operator could adjust the diameter using a joystick and match the diameter of the cell under study.
c. Fully automatic computerized image analysis: In this method, an image could be directly converted to its digital form and analyzed by a computer which was programmed to recognize cell boundaries and calculate the enclosed areas.

The method employed in this study for image analysis was mechanical planimetry.

Image analysis of cells was used to study both water transport and intracellular ice formation in cells. Image analysis of cells involved the evaluation of volumetric shrinkage of cells due to dehydration and evaluation of number of cells that underwent intracellular ice formation. Evaluation was based on the assumption that the cells were regular and spherical.

The change in the diameter of the cell was measured after a dehydration experiment which was hence useful in evaluating the change in volume.

3.3.3.1 Image Analysis to Study Dehydration

During an experiment, usually a cluster of 10-15 cells were focused on, under the microscope. At a given freezing rate, and at different temperatures through the freezing protocol, the diameter of the cells was measured, assuming the cells to be perfectly spherical. When the diameters of the cells decreased, the corresponding volumes of the cells were calculated using the formula $V = 4/3 \times \Pi \times R^3$, where R was the radius of the cell. Hence, the normalized volume (the ratio of the volume at each temperature to the original volume) was evaluated and plotted against temperature for a particular cooling rate.

Finally, by applying non-linear regression analysis and inverse curve fitting techniques, the membrane permeability coefficients could be determined. The details of the study have been presented in the later chapters (Chapters 5 and 6) of this thesis.

3.3.3.2 Image Analysis to Study IIF

Images obtained through the camera were stacked using the software called 'Metacam' to make movies. Usually a cluster of around 30-40 cells were focused on, under the microscope and were examined for blackening. The number of cells that turned black due to IIF at different temperatures through the protocol was noted. Percentage intracellular ice formation (PIIF) was evaluated as the ratio of the number of cells that turned black due to IIF to the total number of cells and was plotted against temperature for different freezing rates.

4. Freezing Response of Pacific Oyster Embryos

4.1 Background

Cryopreservation in aquatic species has been a matter of interest for more than 50 years (He et al 2004, Tiersch 2000). Over the last decade, many researchers have made attempts to study oysters seemingly because; the demand of oysters has been ever growing (He et al 2004, Lin and Lung 1995, Salinas-Flores et al 2008, Salinas-Flores et al 2008). The United States has been the largest producer of oysters in North America. Statistics illustrate that the U.S produces close to production worth $US 100 million. However, the total production has decreased from 1998 due to diseases and adverse weather conditions. The industry has also been continuously plagued with contamination problems that have limited their ability to grow additional problems. At the same time, United States of America have seen their consumption ratio jump from 22 pounds to 30.8 pounds per capita. The following chart provides an idea about the nationwide demand of oyster as a favorite food article (Unic Marketing Group Ltd, NB 2003).

Table 4.1 Average Annual Consumption of Oysters

Table 2. Average Annual Consumption (grams) of Uncooked Oyster			
	Female	Male	Individuals
Age 15 to 44	27.0	109.5	68.3
Age 45 and over	32.0	72.8	50.7
All ages	24.5	74.9	49.1

*Source: 2000 United States Census of American consumption

Table 3. Average Annual Consumption (grams) of Prepared Oyster			
	Female	Male	Individuals
Age 15 to 44	21.4	89.1	55.3
Age 45 and over	25.6	65.4	43.8
All ages	19.7	63.0	40.9

*Source: 2000 United States Census of American consumption

One could assume that newer methods of hatchery production needed to be developed in order to keep up with the growing demand. One possible solution might lie in developing successful cryopreservation protocols for preserving oyster spermatozoa and oocytes/embryos and enabling fertilization. Although there were some exceptions (Hagedorn et al 1996, Lin and Lung 1995, Zhang and Rawson 1996) the study of cryobiology was largely neglected in most aquatic species. Extensive work has been done in studying the membrane permeability characteristics of oyster spermatozoa and oocytes. Hence in this work, attention has been paid to understand the response of pacific oyster embryos to a freezing stress and check the possibility of IIF. Learning that IIF is generally a deleterious event, one might develop a protocol where the optimal freezing rate would be lesser than the one shown to trigger IIF in embryos.

4.2 Sample Preparation

Pacific oyster (Crassostrea gigas) embryos were obtained from a population of fertilized eggs, about 120 minutes after the artificial fertilization in sea water of 34+2% salinity at a temperature of 27$\pm$1 ^{o}C. Hundreds of oyster embryos were pooled from three females. It was only under the microscope, where the females could be distinguished from the males. Seven samples were examined under the microscope among which three were identified as females. The eggs from the females appeared to be larger and more spherical than the sperms from the males. The oyster embryos were found to be spheres with a diameter of ~60μm.

A 10X DPBS (Dulbecco's Phosphate Buffer Saline) solution was used as the cellular suspension with around 50 embryos. These were placed on a petri-dish to be examined under the cryomicroscope for an applied freezing stress. A group of 35-40 embryos were focused on, and a freeze thaw protocol was used to examine their freezing response. The main aim of the experiment was to identify the freezing rates at which the cells showed darkening or flashing to

reveal intracellular ice formation. The freezing protocol used for the experiment has been mentioned in the following section.

4.3 Oyster Experiments at Freezing Rate of 5 ^{o}C/min

4.3.1 Freezing Protocol

Table 4.2 Freezing Protocol for Oyster Embryos at 5 ^{o}C/min

Start temperature (^{o}C)	Rate (^{o}C/min)	End temperature (^{o}C)
23	5	4
4	1	-7
-7	1	-6
-6	5	-40
-40	5	25

4.3.1.1 Description of the Protocol

Before starting the experiments, the oyster embryos had to be provided with iso-osmotic conditions. Hence, the oysters were suspended in 10X DPBS solution which was considered to be iso-osmotic for them. The protocol was decided based on the phase change temperature of 10X DPBS which was calculated using the following formula (Toner et al 1992, Harris et al 1991):

$$1.858 \times \text{osmolality of the solution} = T_{ref} - T_{phase} \ldots\ldots (27)$$

T_{phase} = Phase change temperature of the solution

T_{ref} = Reference temperature which is always taken as 0 ^{o}C

Osmolality is a measure of Osmoles of solute per Kilogram of solution

Osmolality of 10X DPBS was measured using WESCOR's vapor pressure osmometer and was found to be 2820 milli-Osmoles/kg. Learning that extracellular ice formation was probably a necessary condition for intracellular ice formation to occur, it was necessary to know its phase change temperature. Using equation (27), the phase change temperature of 10X DPBS was determined as shown below.

$$1.858 \times 2.82(\text{Osmoles/kg}) = 0\ ^{o}\text{C} - T_{\text{phase change}}$$

$$\text{Or } T_{\text{phase change}} = -5.23956$$

It was thus calculated that the phase change temperature of 10X DPBS was -5.24 ^{o}C approximately. The protocol was started by bringing down the temperature of the cell-suspension from a room temperature of 23 ^{o}C to 4 ^{o}C at a freezing rate of 5 ^{o}C/min, in order to speed up the process. Learning that the phase change of DPBS should have occurred at -5.23 ^{o}C, the suspension was frozen from 4 ^{o}C to -7 ^{o}C at a slower freezing rate of 1 ^{o}C/min and hence it was held at -7 ^{o}C for a minute. Following this, the temperature was raised by a degree to -6 ^{o}C, from where the cell suspension was frozen back to -40 ^{o}C in steps of 5 ^{o}C a minute. Finally, after reaching the end temperature of -40 ^{o}C, the suspension was thawed back to the room temperature at the same freezing rate.

It was believed that this protocol would lead to valuable information regarding the freezing response of Pacific Oyster embryos. The embryos were checked for reduction in size or diameter which would have indicated dehydration or water transport. In addition, the embryos were also checked for intracellular ice formation through sudden blackening o darkening. It is believed that cells undergoing IIF usually demonstrate darkening because of ice formation within them that blocks the passage of light. Blackening or darkening of embryos would be caused by the sudden opaqueness of the embryos due to formation of ice within them.

4.3.2 Observations

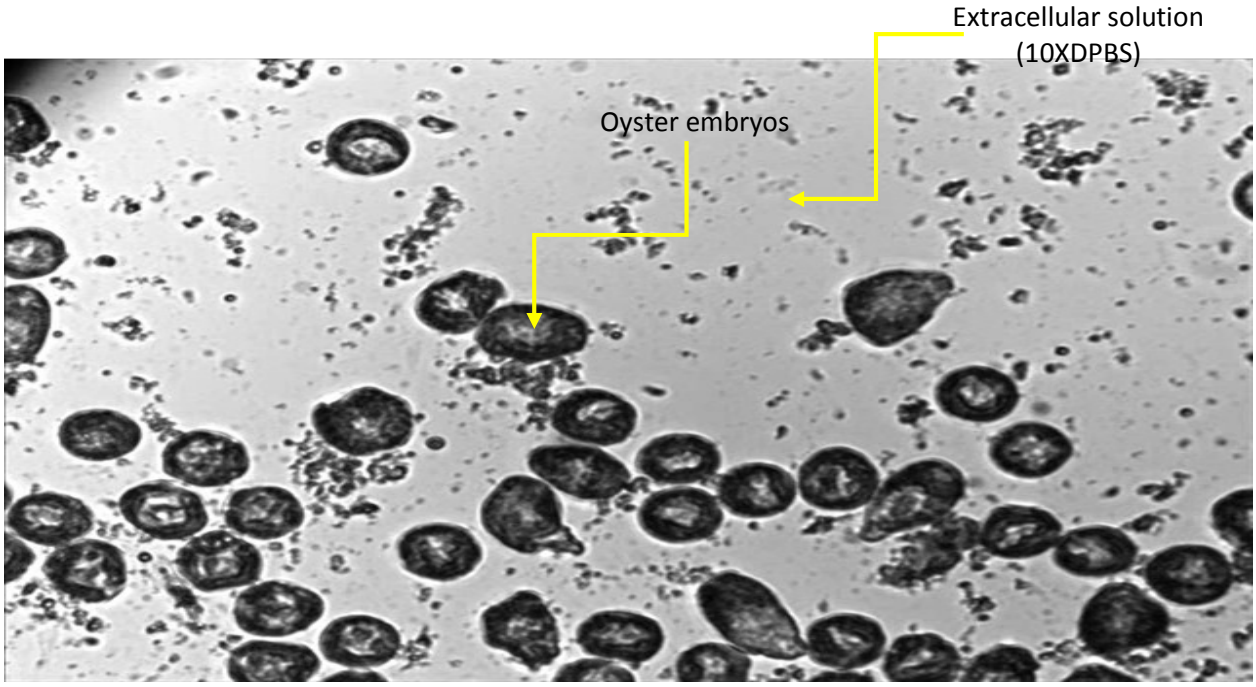

Figure 4.1: The above image shows Pacific Oyster embryos during the course of their freezing at ~ 23 ^{o}C. The extracellular solution appeared to be clear and fluid. During this freezing experiment, a pool of approximately 46 Pacific Oyster embryos was focused on. The embryos appeared to be blackish, yet transparent.

During this experiment, a total of around 46 oyster embryos were focused on. The image was taken at the beginning of the experiment and at room temperature. The oyster embryos were blackish and appeared to be transparent. The room temperature was chosen because it would have given a clear knowledge of how the Pacific Oyster embryos looked when no freezing took place. As mentioned, the extracellular solution of 10X DPBS appeared as clear and fluid. It was learnt that usually intracellular ice formation (IIF) followed extracellular ice formation. Hence attention was paid to understand how the extracellular solution changed its appearance of color during the course of freezing. It was earlier learnt from literatures (Toner et al1990, Toner 1992) that extracellular ice formation was a necessary condition for IIF which would have made observation of extracellular ice formation an important event.

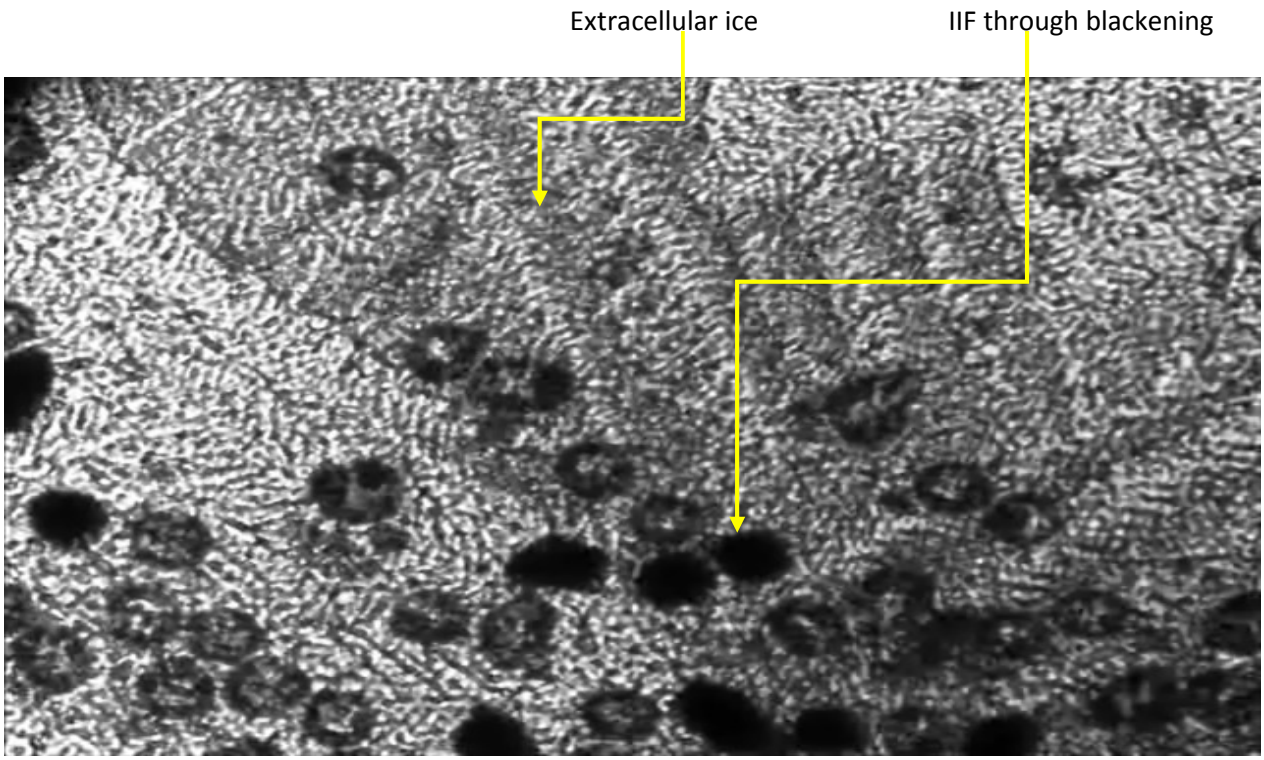

Figure 4.2: The above image was photographed during the course of freezing of the Pacific Oyster embryos at ~ -15 ^{o}C. IIF was seen among some of the embryos through blackening as mentioned earlier. It would be noted that the extracellular solution of 10X DPBS did not appear to be clear and fluid as it did in Figure 4.1.

At about -15 ^{o}C, IIF in oysters was shown through blackening. Ice formed inside the embryos after the extracellular solution turned into ice. Ice formed inside the embryos, didn't let light to pass through the embryos which made them turn black.

Formation of extracellular ice made the above image look hazy. Intracellular ice formation (IIF) immediately followed extracellular ice formation. It could be seen that around 10 out of 40 oyster embryos turned black due to formation of intracellular ice. Formation of extracellular ice was probably a necessary condition for IIF in the embryos. Percentage intracellular ice formation (PIIF) was evaluated as the ratio of the number of embryos that turned black (showing IIF) to the total number of embryos that were present in the field of view and were being used in the freezing experiment.

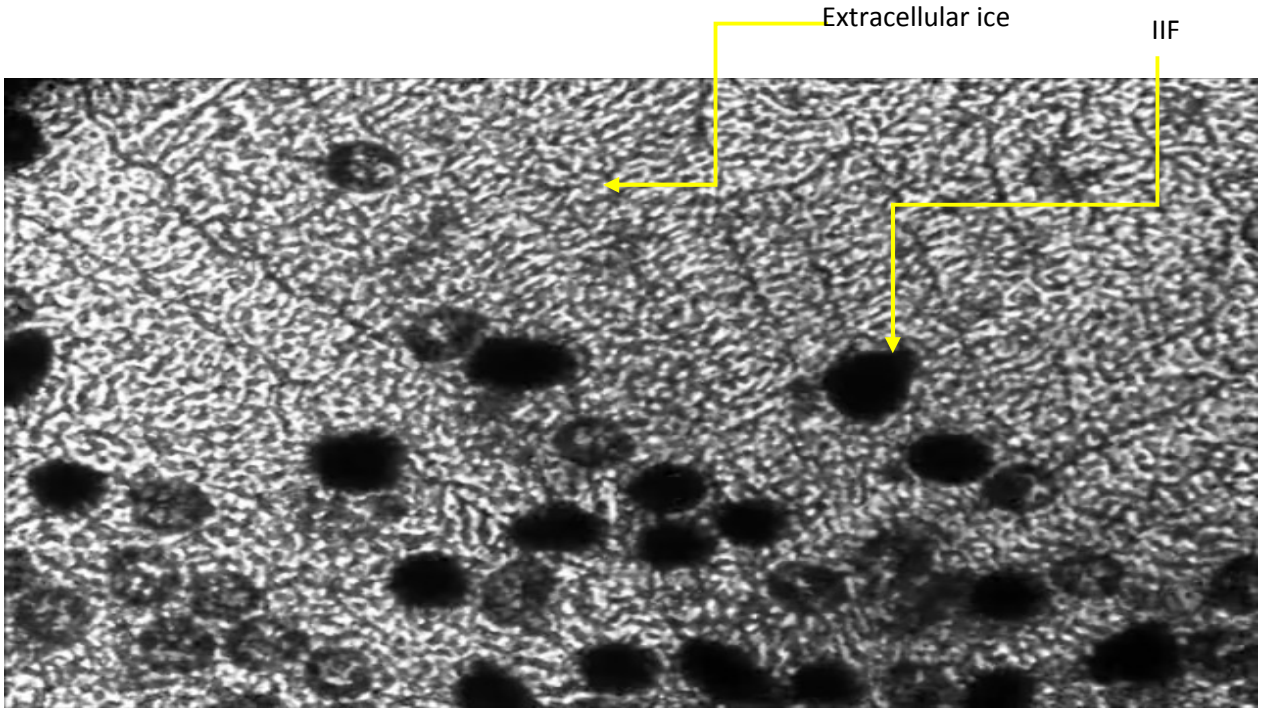

Figure 4.3: Above image was photographed during the course of freezing of the Pacific Oyster embryos at ~ -18 ^{o}C. IIF was seen among some of the embryos through blackening. It might be seen that ~ 23 out of 46 embryos underwent IIF through blackening.

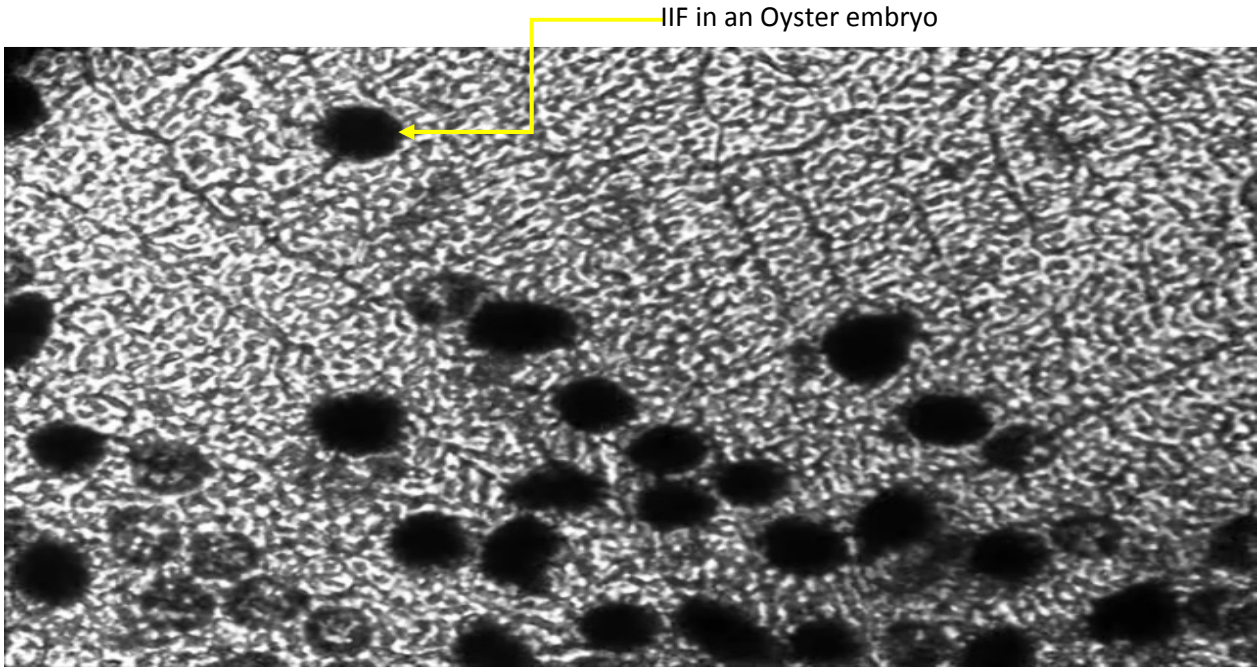

Figure 4.4: Above image shows Oyster embryos at ~ -19 ^{o}C. It was seen that approximately 36 embryos turned black at a freezing rate of 5 ^{o}C/min. Percentage intracellular ice formation(PIIF) was evaluated as a ratio of 36 to 44 and was approximately 80%

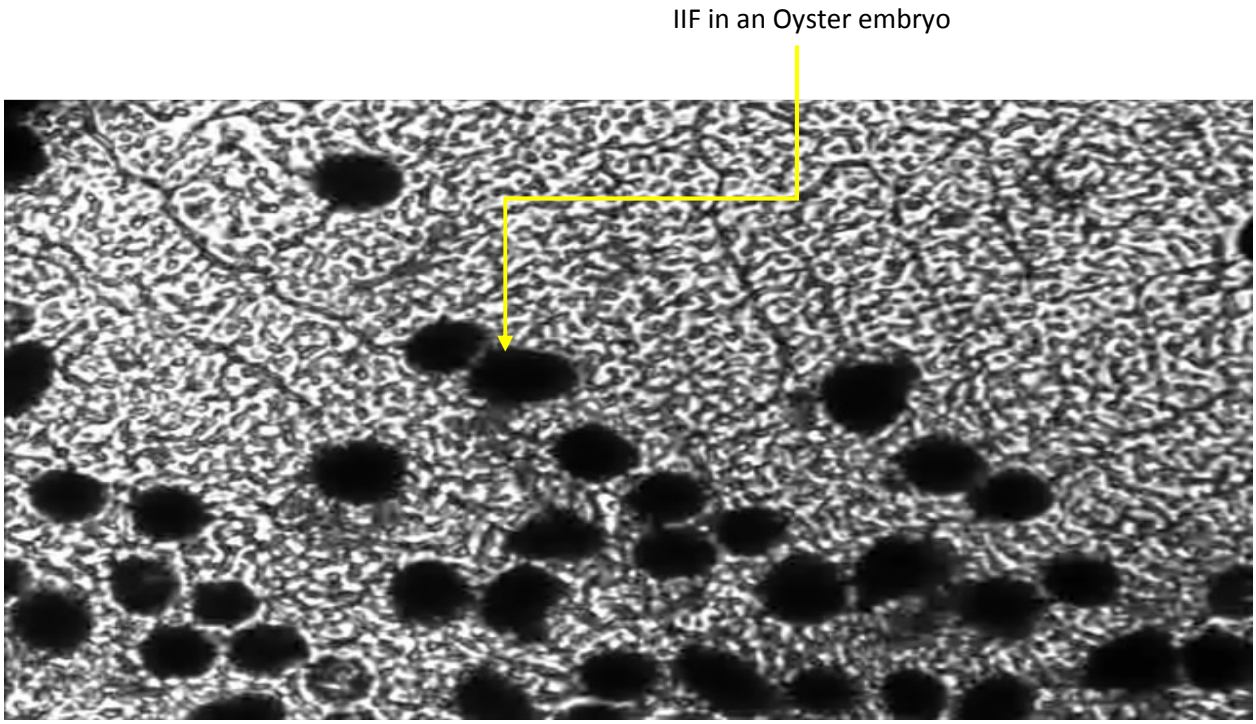

Figure 4.5: Above image shows Oyster embryos at ~ -19.9 ^{o}C. Approximately all 46 embryos turned black at a freezing rate of 5 ^{o}C/min. Thus, PIIF ~ 100%

4.3.3 Results

Table 4.3 Temperature vs PIIF for Oyster Embryos at 5 ^{o}C/min

Temperature (^{o}C)	Percentage IIF(PIIF)
-6	0
-7.8	8.69
-8.5	10.86
-9.75	13.04
-11.5	17.39
-11.9	19.56
-14.5	21.73
-15.6	28.26

Table 4.3 continued

Temperature (°C)	Percentage IIF(PIIF)
-16.7	32.6
-17.8	45.65
-18.8	78.26
-19	86.9
-19.9	100

IIF started at around -8 °C till about -20 °C when almost all of the embryos under observation turned black under the cryomicroscope showing IIF. Hence, a plot of temperature against percentage intracellular ice formation was made at the given freezing rate of 5 °C/min.

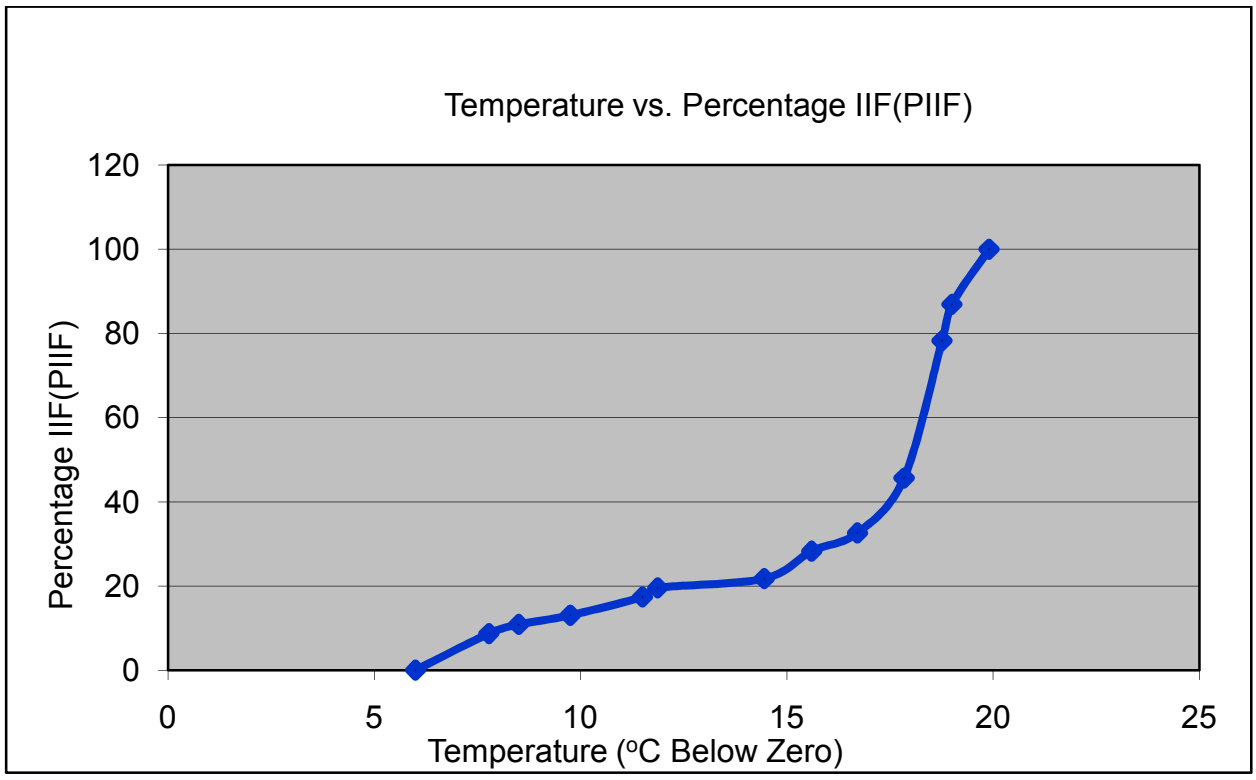

Figure 4.6: Variation of PIIF with decreasing temperature

4.4 Oyster Experiments at Freezing Rate of 10 ^{o}C/min

4.4.1 Freezing Protocol

Table 4.4 Freezing Protocol for Oyster Embryos at 10 ^{o}C/min

Start temperature (^{o}C)	Rate (^{o}C/min)	End temperature (^{o}C)
25	10	4
4	1	-7
-7	1	-6
-6	10	-40
-40	10	25

4.4.1.1 Description of the Protocol

The oyster embryos were provided with iso-osmotic conditions. Hence, the oysters were suspended in 10X DPBS solution which was considered to be iso-osmotic for them. The protocol was decided based on the phase change temperature of 10X DPBS which was calculated using the following formula (Toner wt al 1992, Harris et al 1991):

$$1.858 \times \text{osmolality of the solution} = T_{ref} - T_{phase} \ldots\ldots (27)$$

T_{phase} = Phase change temperature of the solution

T_{ref} = Reference temperature which is always taken as 0 ^{o}C

As mentioned before, measured osmolality was the number of Osmoles of the solute per Kilogram of the solvent. Osmolality of 10X DPBS was measured using WESCOR's vapor pressure osmometer and was found to be 2820 milli-Osmoles/kg. Learning that extracellular ice formation was probably a necessary condition for intracellular ice formation to occur, it was

necessary to know its phase change temperature. Using equation (27), the phase change temperature of 10X DPBS was determined as shown below.

$$1.858 \times 2.82(\text{Osmoles/kg}) = 0\ ^{o}\text{C} - T_{\text{phase change}}$$

$$\text{Or } T_{\text{phase change}} = -5.23956$$

The phase change temperature of 10X DPBS was theoretically predicted as ~ -5.24 ^{o}C approximately. The protocol was now started by bringing down the temperature of the cell-suspension from a room temperature of 23 ^{o}C to 4 ^{o}C at a freezing rate of 10 ^{o}C/min, in order to speed up the process. Learning that the phase change of DPBS should have occurred at -5.23 ^{o}C, the suspension was frozen from 4 ^{o}C to -7 ^{o}C at a slower freezing rate of 1 ^{o}C/min and hence it was held at -7 ^{o}C for a minute. Following this, the temperature was raised by a degree to -6 ^{o}C, from where the cell suspension was frozen back to -40 ^{o}C in steps of 10 ^{o}C a minute. Finally, after reaching the end temperature of -40 ^{o}C, the suspension was thawed back to the room temperature at the same freezing rate.

Similar to the earlier experiment on Pacific Oyster embryos at 5 ^{o}C/min, it was believed that this protocol would lead to information regarding the freezing response of Pacific Oyster embryos. Once again, the embryos were checked for reduction in size or diameter which would have indicated dehydration or water transport. In addition, the embryos were also checked for intracellular ice formation through sudden blackening or darkening. The experiment at freezing rate of 10^{o}C/min was done in order to corroborate the outcome of the earlier experiment at 5^{o}C/min. The fact that Oyster embryos underwent IIF at 5 ^{o}C/min probably meant that this freezing rate was “too fast” for them. It should also have indicated towards obtaining similar results at a higher freezing rate, such as 10 ^{o}C/min. The next set of experiments were performed with Pacific Oyster embryos from the same sample at 10 ^{o}C/min.

4.4.2 Observations

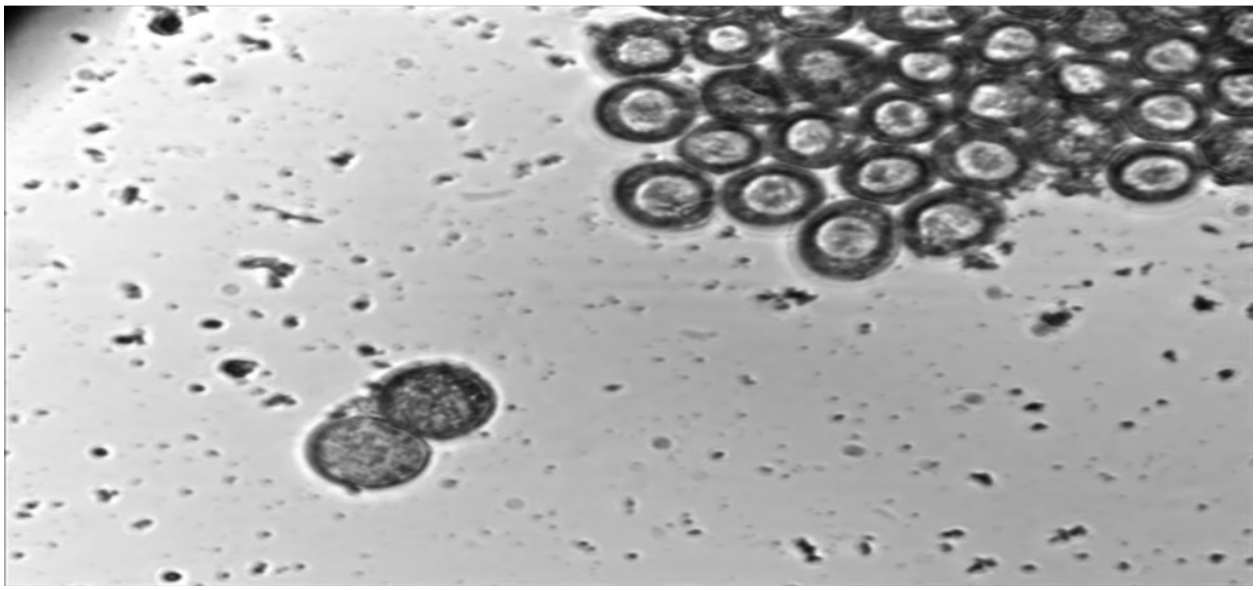

Figure 4.7: The above image shows Pacific Oyster embryos during the course of their freezing at ~ 25 ^{o}C. The extracellular solution appeared to be clear and fluid. During this freezing experiment, a pool of around 32 Pacific Oyster embryos was focused on. The embryos appeared to be blackish, yet transparent.

During freezing, the freezing rate was changed from 5 ^{o}C/min to 10 ^{o}C/min. The image was chosen for report in order to have a clear knowledge of the appearance of the oysters and the extracellular solution at the start of the freezing process. It was learnt from the earlier experiment that IIF in cells was visible through conspicuous blackening, and it followed extracellular ice formation in the vicinity of -5.23 ^{o}C. The phase change temperature was learnt through calculations performed in section 4.3.1.1. Thus, attention was paid in order to observe any change in coloration or appearance of the extracellular solution and the oyster embryos. Percentage intracellular ice formation was evaluated as the ratio of the number of embryos that turned black during the course of freezing to the total number of embryos used in the experiment. Thus much attention was paid to observe extracellular ice formation that would have preceded intracellular ice formation (IIF).

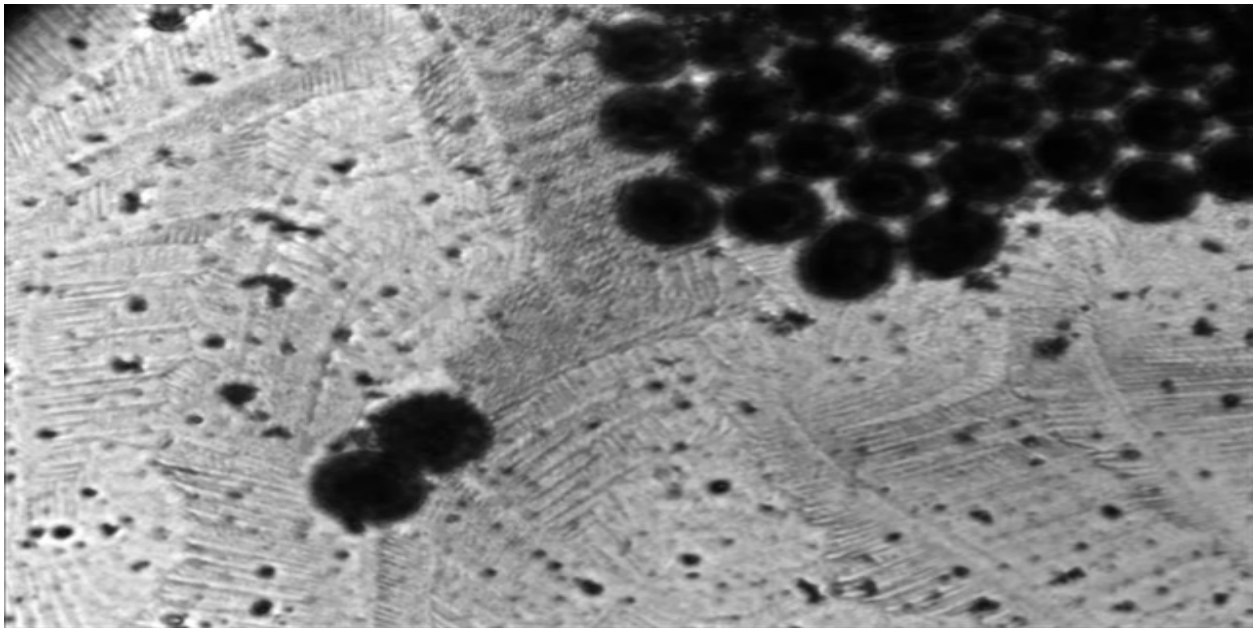

Figure 4.8: The above image shows IIF of oyster embryos at -18 ^{o}C approximately. It was seen that approximately all 32 embryos turned black at a freezing rate of 10 ^{o}C/min. Thus, PIIF ~ 100%

4.4.3 Results

Table 4.5 Temperature vs PIIF for Oyster Embryos at 10 ^{o}C/min

Temperature (^{o}C)	Percentage IIF(PIIF)
-6	0
-6.65	3.13
-7.8	6.25
-8.5	9.38
-9.75	12.5
-10.6	15.63
-11.2	18.75
-12.4	21.88

Table 4.5 continued

Temperature (^{o}C)	Percentage IIF(PIIF)
-14	25
-16.2	34.38
-17	37.5
-17.4	40.63
-17.6	43.75
-18	100

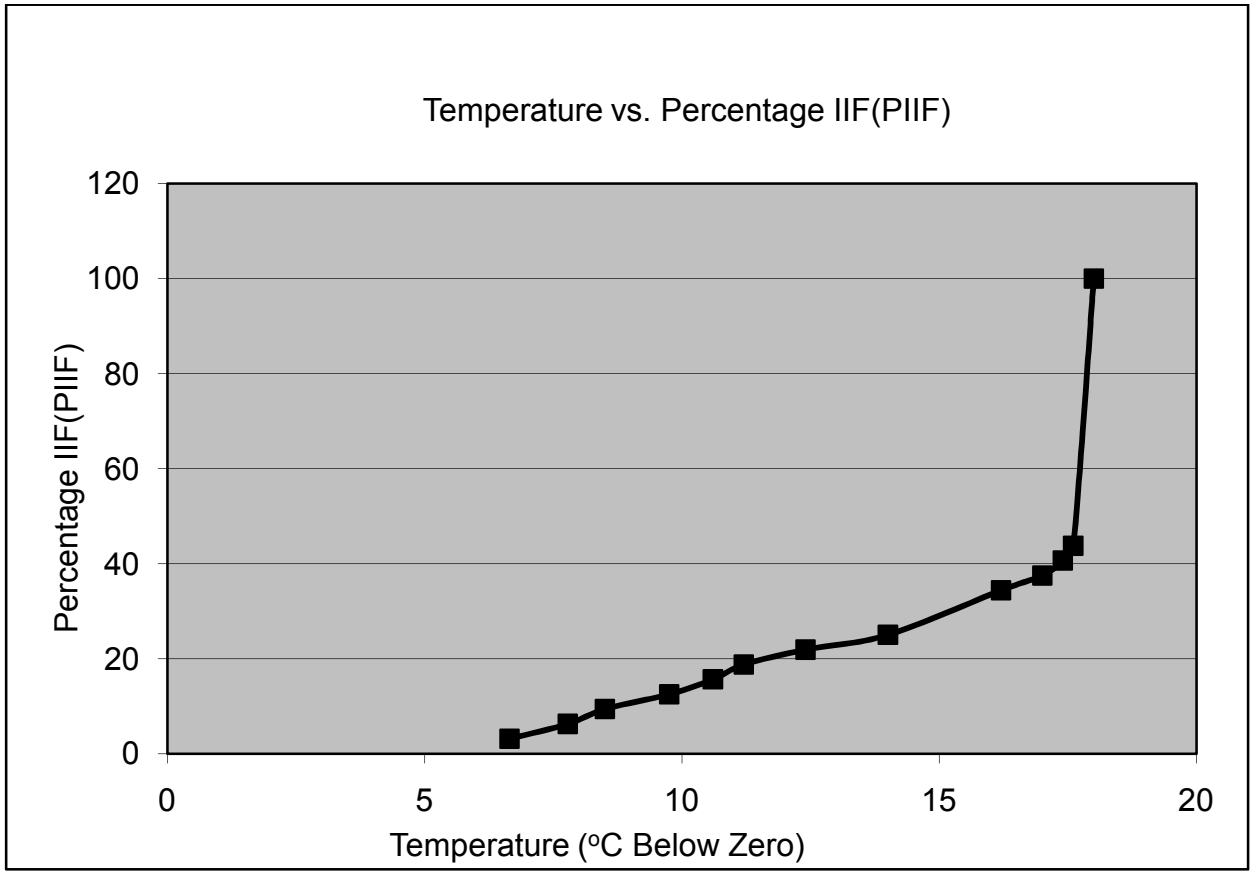

Figure 4.9: Above plot shows the variation of percentage intracellular ice formation with decreasing temperature obtained experimentally. Percentage intracellular ice formation was evaluated as the ratio of the number of embryos that showed darkening to the total number of embryos in a field of view under the cryomicroscope.

4.5 Discussions and Conclusion

It is believed that intracellular ice formation (IIF) is generally a deleterious event, which might be lethal to cell survival. Hence, working on the same lines, the idea of analysis was to identify the freezing rates at which intracellular ice formation occurred in oyster embryos. This would probably reveal that under the given conditions, the used freezing rate was "too fast" for the oyster embryos, and could provide information and aid future researchers in successful designing of cryopreservation protocols. However, due to non-availability of oysters during most part of the season, only two different freezing rates (5 and 10 ^{o}C/min), could be employed for experiments. IIF was observed at both the freezing rates. At 5 ^{o}C/min, IIF in oysters occurred between -6 ^{o}C and -20 ^{o}C approximately, when all the embryos underwent IIF. At 10 ^{o}C/min, IIF occurred between -6 ^{o}C and -18 ^{o}C.

In order to develop a successful cryopreservation protocol, further experimentation is required at lower freezing rates. The fact that IIF was observed at a freezing rate as low as 5 ^{o}C/min, probably indicates that an optimal freezing rate exists below this rate and hence needs to be evaluated. The evaluation of an optimal freezing rate would require experimentation at lower freezing rates such as 1 ^{o}C/min or below. The optimal cooling rate of a biological cell has been defined as the highest cooling rate at which 5 % of intracellular water is retained and at an end temperature of ~ -15 ^{o}C (Thirumala and Devireddy 2005).

5. Freezing Response of Jurkat Cells

5.1 Background

In the earlier chapters of this thesis, experiments based on evaluation of freezing responses of cells have been performed in order to develop a cryopreservation procedure. However, such experiments could also be done in order to evaluate the freezing response of certain malignant cells which might be useful to develop a cryodestruction procedure in an attempt to decimate them. In this work, freezing response of Jurkat cells was studied with the same intent.

Jurkat cells are derived cell lines from human T-cell leukemia and are used for determining the mechanism of differential susceptibility to anti cancer drugs and radiation (Barmak et al 2003). Substantial work has been done in the field of cryobiology to study prostate tumor cells (Wolkers et al 2007), breast cancer cells (Hong and Rubinsky 1994) and uterine fibroid tumor tissues (Devireddy et al 2001). To the best of our knowledge, not much work with the exception of Thirumala et al (Thirumala et al 2007) has been done in order to evaluate the freezing response of these cells. Probably Jurkat cells are relatively less understood. The main idea of working on these cells was to evaluate the optimal freezing rate for these cells. In order to check the validity of the result, these cells were frozen at higher freezing rates and checked for occurrence of IIF.

5.2 Sample Preparation

Jurkat cells were maintained in 25 cm^2 T-flasks (BD Falcon, Franklin Lanes, NJ) with 5 ml of HyQ® RPMI-1640-reduced serum medium (RPMIRS) supplemented with 3% fetal bovine serum (FBS) and incubated at 37 ^oC in a humidified atmosphere containing 5% CO_2. For

cryomicroscopy experiments, Jurkat cells were transferred to a centrifuge tube and were spun down at 1900 rpm for 5 minutes using Eppendorf Minispin Plus centrifuge. The pellet was resuspended in 1X Dulbecco's Phosphate Buffered Saline (DPBS) solution, which was considered isotonic for these cells.

5.3 Jurkat Experiments at 1 ^{o}C/min

Experiments on Jurkat cells were performed at various freezing rates in order to observe their response, apparently at both "slow" and "fast" freezing rates. At first, a freezing rate of 1 ^{o}C/min was chosen that seemingly was a "slow" freezing rate for most cells. It was interesting to see if the cells underwent dehydration at this freezing rate. Later experiments were performed at various freezing rates between 1 ^{o}C/min and 50 ^{o}C/min and the freezing response of Jurkat cells was studied using cryomicroscopy.

5.3.1 Freezing Protocol at 1 ^{o}C/min

Table 5.1 Freezing Protocol for Jurkat Cells at 1 ^{o}C/min

Start temperature (^{o}C)	Rate (^{o}C/min)	End temperature (^{o}C)
21	10	4
4	1	-20

5.3.1.1 Description of the Protocol

It has been shown that 1^{o}C/min is generally a "slow cooling rate" for most cells (Mazur 1970). The protocol was designed anticipating water transport in Jurkat cells in order to evaluate its membrane permeability characteristics at this rate. The membrane permeability characteristics would have helped in evaluating the optimal freezing rate for these cells. As mentioned in Chapters 1 and 3, water transport is governed by a difference in chemical potentials between the

extracellular solution and the intracellular water. It might be recollected that the chemical potential of the extracellular solution changed with extracellular ice formation, which established a difference in potential between it and the supercooled water inside the cell. It was thus essential to calculate the phase change temperature of the extracellular solution and to reach it at a "slow freezing rate." The phase change temperature was calculated as -0.6 ^{o}C approximately, using equation (27). In order to speed up the process, the temperature was brought down from 21 ^{o}C to 4 ^{o}C at a rate of 10 ^{o}C/min. Freezing rate was slowed down to 1 ^{o}C/min till an end temperature of -20 ^{o}C, with an anticipation of watching cell dehydration.

5.3.2 Observation

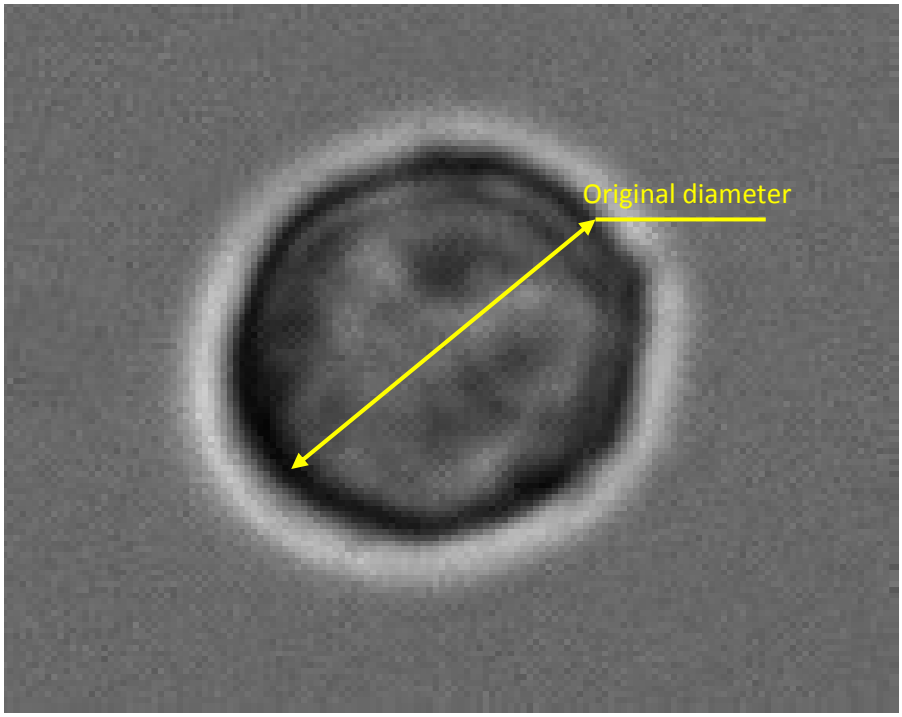

Figure 5.1: The above image shows a Jurkat cell at ~ 21 ^{o}C. This image was chosen in order to learn about the appearance of the cell under microscope at room temperature. The shape of Jurkat cell was considered spherical with a diameter of 12 µm approximately as measured earlier by other researchers (Thirumala et al 2007). The diameter from the image was measured using a linear scale and was used as reference for the other images obtained during the course of freezing. Percentage shrinkage was evaluated as a ratio of the diameter from subsequent images to the diameter measured from this image.

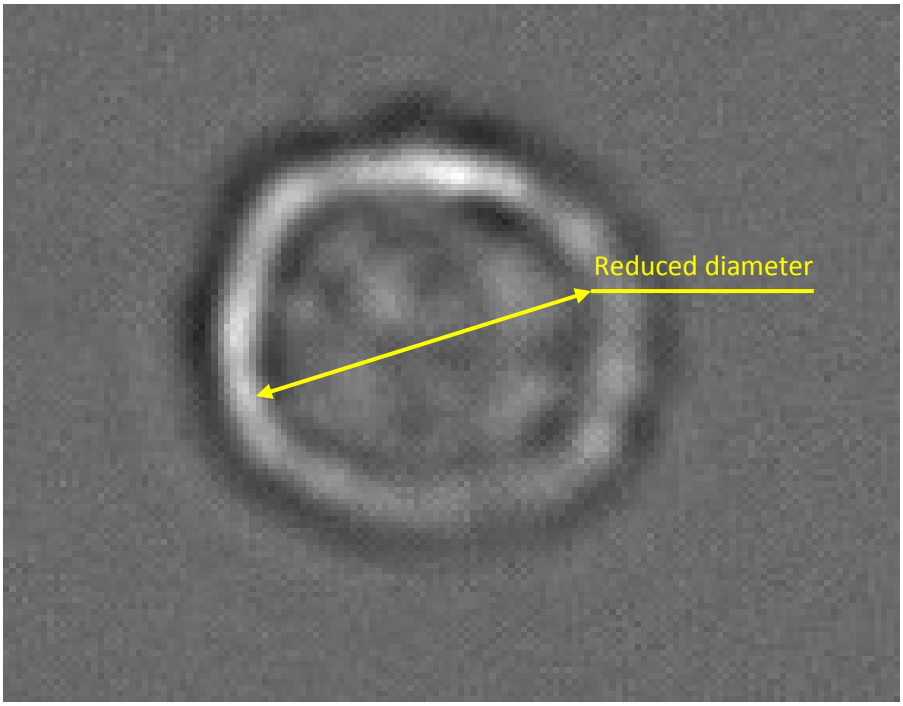

Figure 5.2: The above picture shows the same Jurkat cell at -2 ^{o}C. As mentioned earlier, the cell was assumed to be spherical. Hence, the normalized volume (the ratio between the volume of the cell at this temperature to the original volume at room temperature) could be obtained by evaluating the ratio between the areas at corresponding temperatures and raising the ratio by a power of 1.5 subsequently. It could be noted from the above image that the cell reduced in area.

The normalized volume of any reduced cell is the subject of interest in water transport studies. Attention was paid to notice any change in the diameter or the surface area of the cell. Assuming a Jurkat cell to be spherical, the diameter of the cell was noted as 12 +/- 1.1 μm from the work of earlier researchers (Thirumala et al 2007). However, the subject of interest being just a ratio, this value wasn't used in calculation of normalized volume. The normalized volume of the Jurkat cell at a temperature of ~ -2 ^{o}C was evaluated as a ratio of the diameter at this temperature to the original diameter of the cell at ~ 21 ^{o}C. This ratio was calculated as 0.76 approximately. This revealed that there might have been loss of water from the cell that led to shrinkage in volume.

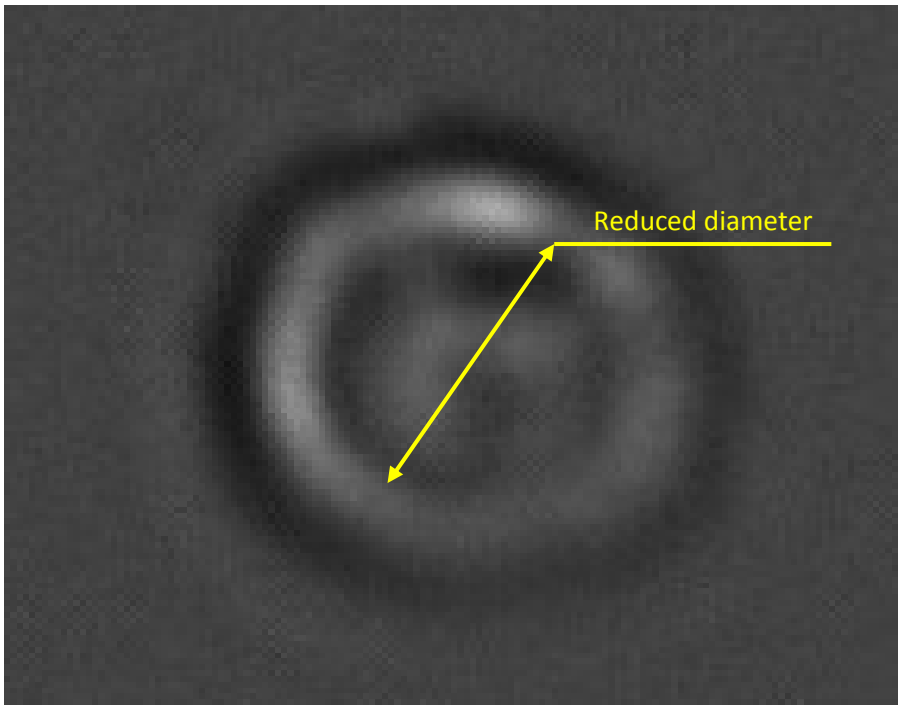

Figure 5.3: The above image shows the same Jurkat cell at ~ -7 ^{o}C. The normalized volume of the cell at this temperature was evaluated as 0.52.

Images at lower temperatures till -10 ^{o}C were analyzed for reduction in volume. Apparently, the normalized volume remained fixed at the above mentioned value. The cell did not seem to shrink any further. It probably suggested that the cell did not lose all the intracellular water. It was known from numerous earlier literatures that a fraction of cellular volume did not participate in cellular dehydration (Mazur 1963, Mazur 1970, Mazur 1977, Mazur 1984, and Toner et al 1990), that such a portion of cellular volume was known as inactive cell volume. Researchers (Thirumala et al 2007) evaluated the inactive cell volume of Jurkat cell as 0.52 and the observations from this work were seemingly in good agreement.

Learning from these observations, it was necessary to plot a curve between normalized volume and different subzero temperatures as the first step towards learning about the freezing response of Jurkat cells at the given freezing rate of 1 ^{o}C/min.

5.3.3 Experimental Results

The following table shows the experimental data obtained at freezing rate of 1 ^{o}C/min. As mentioned earlier, the cells were frozen in an extracellular medium of 1X DPBS which was considered as isotonic for them. The phase change temperature of 1X DPBS was calculated as ~ -0.6 ^{o}C. It was noted that till -0.53 ^{o}C, there was no significant change in the diameter of the cell. Hence, the first observation was taken from -0.5 ^{o}C. The normalized volume was obtained at each subzero temperature till ~ -10 ^{o}C. It was noted that the normalized volume remained fixed (0.52) from -6 ^{o}C through this temperature.

Table 5.2 Temperature vs Normalized Volume of Jurkat Cell at 1 ^{o}C/min

Temperature (^{o}C)	Normalized volume (V/V_o)
-0.53	1
-1	0.93
-2	0.76
-3	0.58
-4	0.56
-5	0.54
-6	0.52
-7	0.52
-8	0.52
-9	0.52
-10	0.52

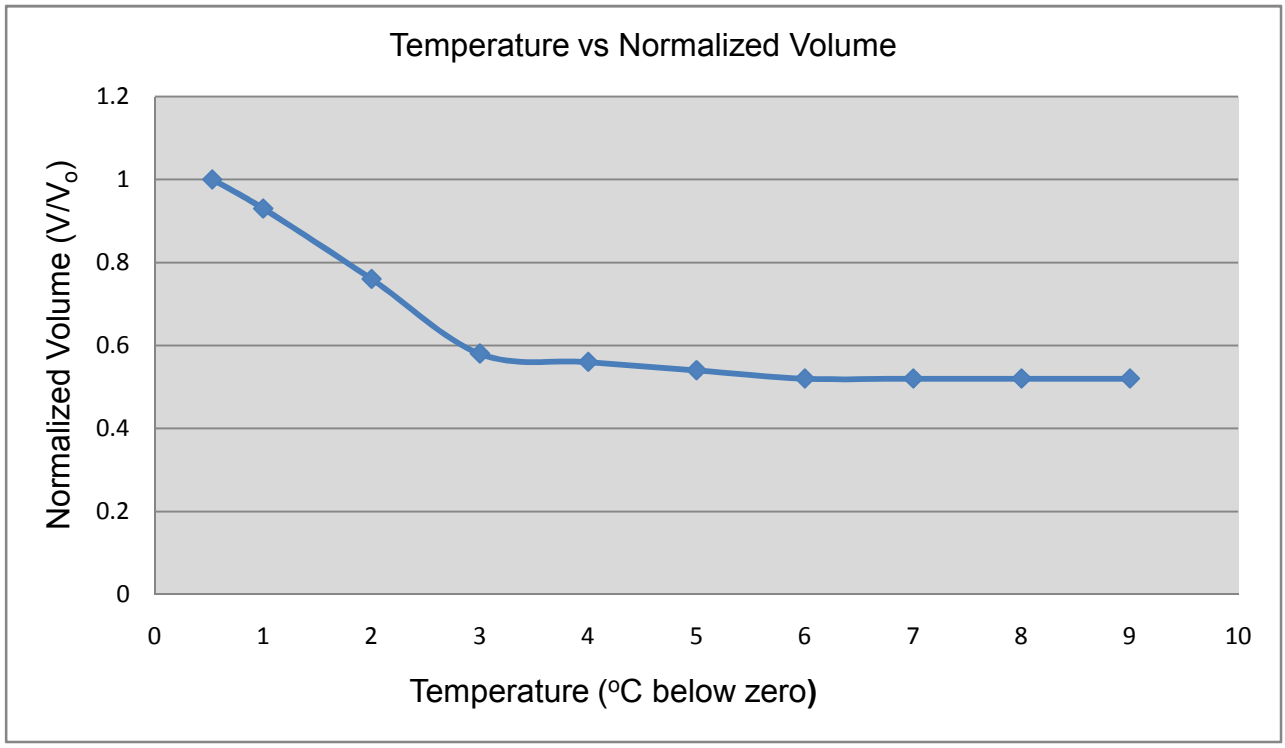

Figure 5.4: Variation of normalized volume with decreasing temperature

The normalized volume is the ratio of the volume at a particular temperature to the original volume. Apparently the cell did not shrink beyond a particular value of normalized volume, which was the inactive cell volume. The inactive cell volume for Jurkat cells was evaluated as 52% of the original cell volume.

5.3.4 Numerical Simulations

5.3.4.1 Water Transport Model

$$\frac{dV}{dT} = -\frac{L_P A R T}{v_w B}\left[\ln\frac{(V - V_b)}{(V - V_b) + v_w(n_s)} - \frac{\Delta H_f}{R}\left(\frac{1}{T_R} - \frac{1}{T}\right)\right] \ldots . (13)$$

$$L_P = L_{Pg}\exp\left[\frac{E_{Lp}}{R}\left(\frac{1}{T} - \frac{1}{T_R}\right)\right] \ldots . (14)$$

The above equations are collectively known as the water transport equations. The water transport equation represents the change in volume of a cell (during dehydration) as a function of temperature. The right hand side of the equation represents the driving force as the difference between the chemical potentials of intracellular water and extracellular solution. In order to obtain L_{pg} and $E_{Lp,}$ it was necessary to have accurate information about V_b. The experimental result for inactive cell volume ($V_b \sim 0.52$) agreed with earlier obtained results (Thirumala et al 2007), as shown below.

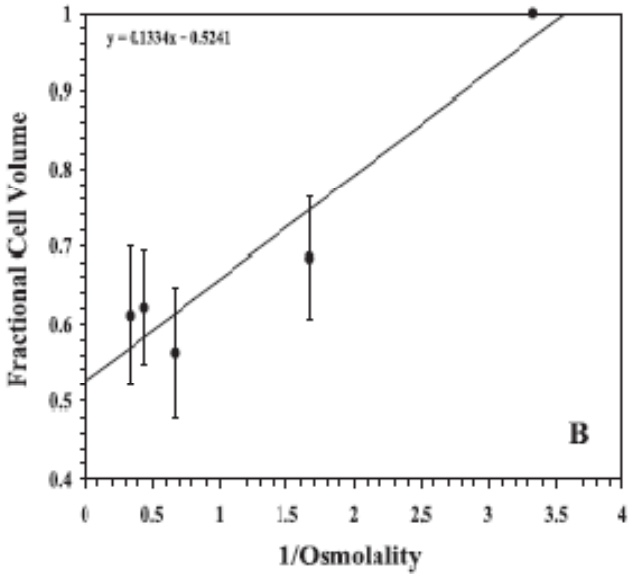

Figure 5.5 Y-intercept reveals inactive cell volume of Jurkat cells (0.52) (Thirumala et al 2007)

The Boyle-Van't Hoff plot showed the changes in volume of Jurkat cells when they were subjected to varying osmolalities (0.3, 0.6, 1.5, 2.25 and 3.00 Osm/kg) at temperature ~ 27 ^{o}C.

The biophysical parameters for water transport were hence estimated using a non linear regression algorithm as previously reported (Thirumala et al 2003, Thirumala et al 2005, and Thirumala et al 2006). The experimentally measured water transport data at 1 ^{o}C/min for Jurkat cells were compared to theoretically predicted curves (equations (13) and (14)).The biophysical

parameters of water transport were iteratively adjusted until the chi squared variance, χ^2, was minimized or a goodness-of-fit parameter, R^2, was maximized, (A value of 1 for R^2 would represent a perfect fit while a value of 0, a flawed fit.) using a gradient search method described in Bevington and Robison (Bevington and Robinson, 1992). All reported parameters were obtained for an $R^2 > 0.95$.

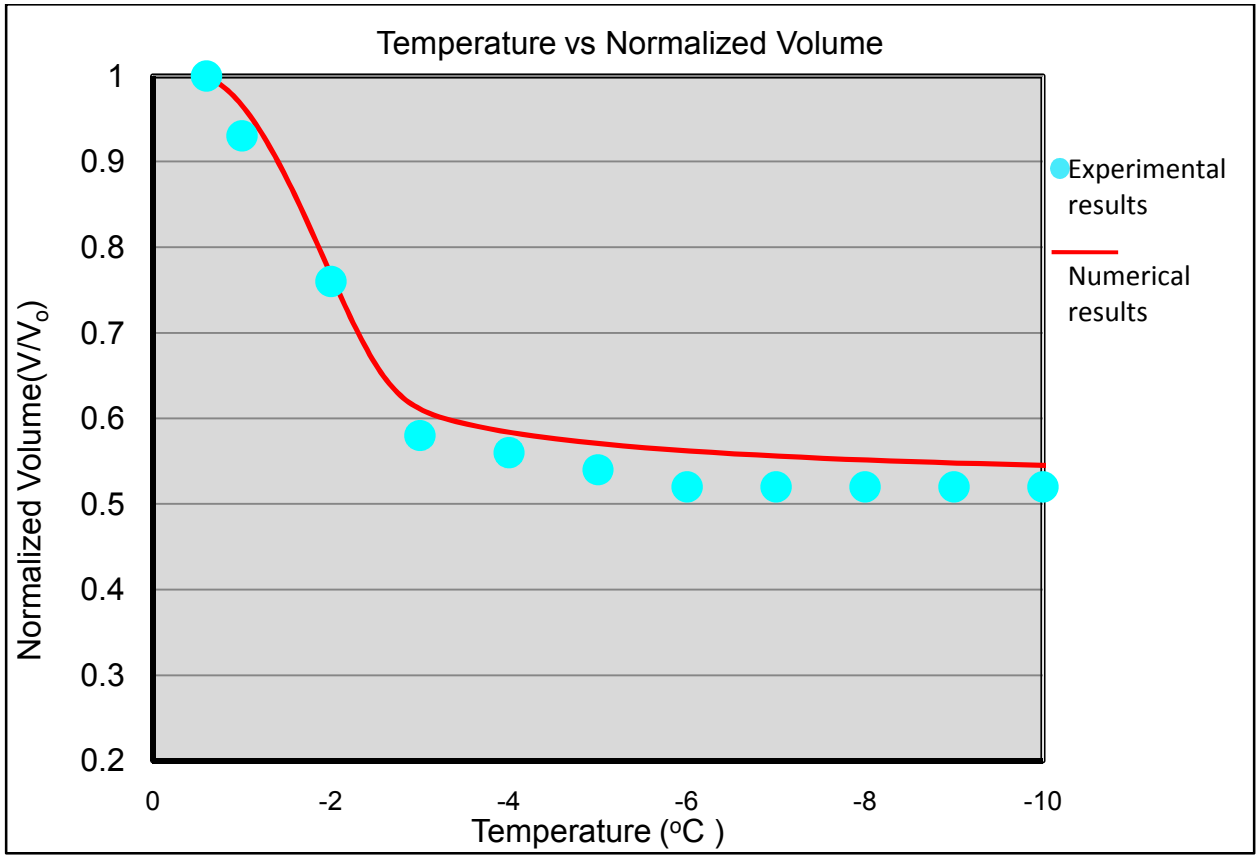

Figure 5.6: Numerical simulation of volume shrinkage during water transport

The above plot shows a comparison between the experimentally obtained and the numerically simulated values of normalized volume of Jurkat cells dehydrated using a freezing rate of 1 ^{o}C/min. Thus, using the non linear regression algorithm, the values of L_{pg} and E_{Lp} were obtained which were used to numerically simulate the volume shrinkage at various temperatures within the protocol. The obtained values of $L_{pg\ and}$ E_{Lp} were hence used to determine the optimal

freezing rate for Jurkat cells. In order to find out the optimal freezing rate, the generic optimal cooling rate equation was used which was derived by Thirumala and Devireddy in 2005.

5.3.4.2 Generic Optimal Cooling Rate Equation (GOCRE)

$$B_{optimal} = 1009.5 * \exp^{(-0.0546 * E_{Lp})} * (L_{pg}) * \frac{SA}{WV}$$

SA = surface area of the cell membrane

WV = Volume of water contained within the cell = $V_o - V_b$

L_{pg} = Reference permeability of cell membrane

E_{Lp} = Activation energy of permeation process

Using the above equation, the following results were obtained:

Cell	**L_{pg} (µm/min-atm)**	**E_{Lp} (Kcal/mole)**	**R^2**	**$B_{(opt)}$ (^{0}C/min)**
Jurkat	0.04	69.7	0.96	1.3

5.4 Jurkat Experiments at 10 ^{o}C/min

The freezing experiment on Jurkat cells at 1 ^{o}C apparently revealed that it was a "slow cooling rate" for these cells that caused them to dehydrate. The results obtained through the earlier experiments helped one obtain the optimal freezing rate. It was now to be seen if higher

freezing rates caused these cells to form ice intracellularly. Hence, a higher freezing rate of 10 ^{o}C was chosen and several experiments were performed using this rate subsequently.

5.4.1 Freezing Protocol at 10 ^{o}C/min

Table 5.3 Freezing protocol for Jurkat Cells at 10 ^{o}C/min

Start temperature (^{o}C)	Rate (^{o}C/min)	End temperature (^{o}C/min)
21	10	4
4	1	-2.6
-2.6	1	-1.6
-1.6	10	-30
-30	10	25

5.4.1.1 Description of the Protocol

Freezing process was started at the room temperature of 21 ^{o}C/min. The temperature of the sample was quickly brought down from 21 ^{o}C to 4 ^{o}C at a rate of 10 ^{o}C/min in order to save time. Hence, the temperature was reduced from 4 ^{o}C to -2.6 ^{o}C at 1 ^{o}C/min because -0.6 ^{o}C (calculated using equation (27)) was the phase change temperature of 1X DPBS and extracellular ice formation was expected around that temperature. The temperature was slightly elevated above -2.6 ^{o}C in order to observe the phase change temperature and hence the actual freezing protocol started by freezing the cells from around -1.6 ^{o}C to -30 ^{o}C at the desired freezing rate of 10 ^{o}C/min. During the course, IIF was observed through blackening of cells which followed the formation of extracellular ice. Hence special attention was given in order to observe the formation of extracellular ice. Finally the cells were thawed back to the room temperature at a thawing rate of 10 ^{o}C/min.

5.4.2 Observation

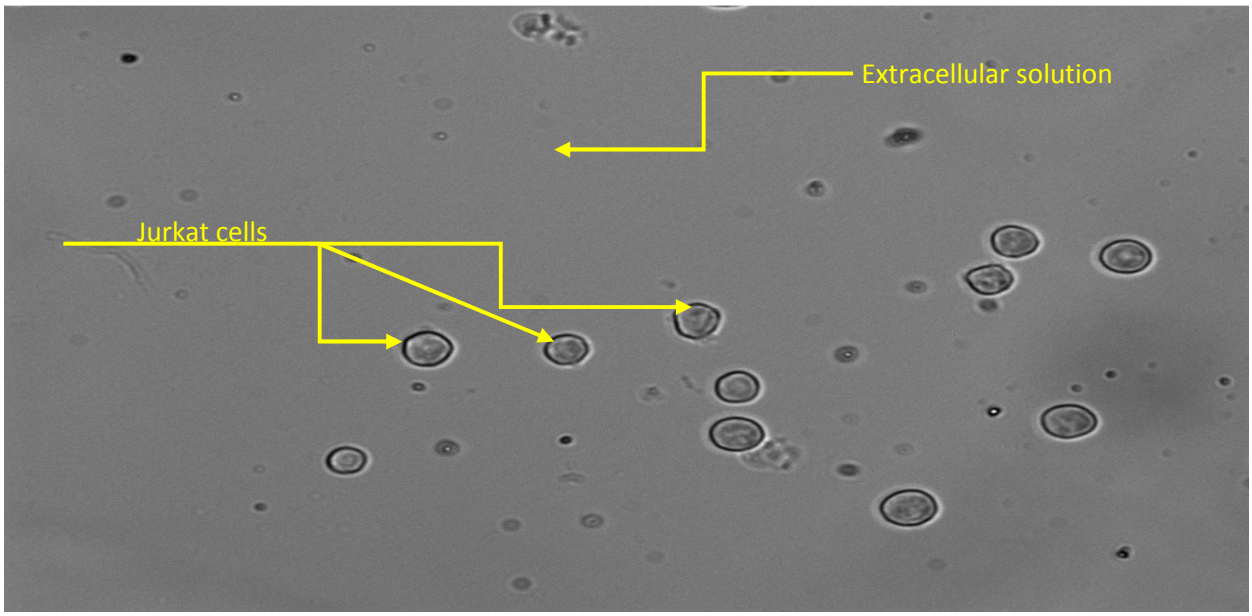

Figure 5.7: The above image shows approximately 12 Jurkat cells in 1X DPBS solution at ~ 21 ^{o}C. The image was chosen for report in order to have a clear knowledge of how Jurkat cells appeared before freezing process started.

During the start of the freezing process, twelve Jurkats cells were focused on with an intention of observing their freezing response at a freezing rate of 10 ^{o}C/min. In the above image, it could be seen that the Jurkat cells appeared grayish and transparent. The extracellular solution of 1X DPBS appeared to be clear and fluid. At a freezing rate of 10 ^{o}C/min, much attention would be paid in order to observe any change in appearance of the extracellular solution, learning that extracellular ice formation was probably a necessary condition for intracellular ice formation (IIF). It was learnt from previous literatures (Toner et al 1990, and Toner 1993) that extracellular ice through some yet unknown mechanism would transform the interior surface of the plasma membrane into an effective nucleator which thus would lead to seeding of supercooled intracellular water into ice. Subsequently, the cells undergoing freezing would also be examined for any change in coloration.

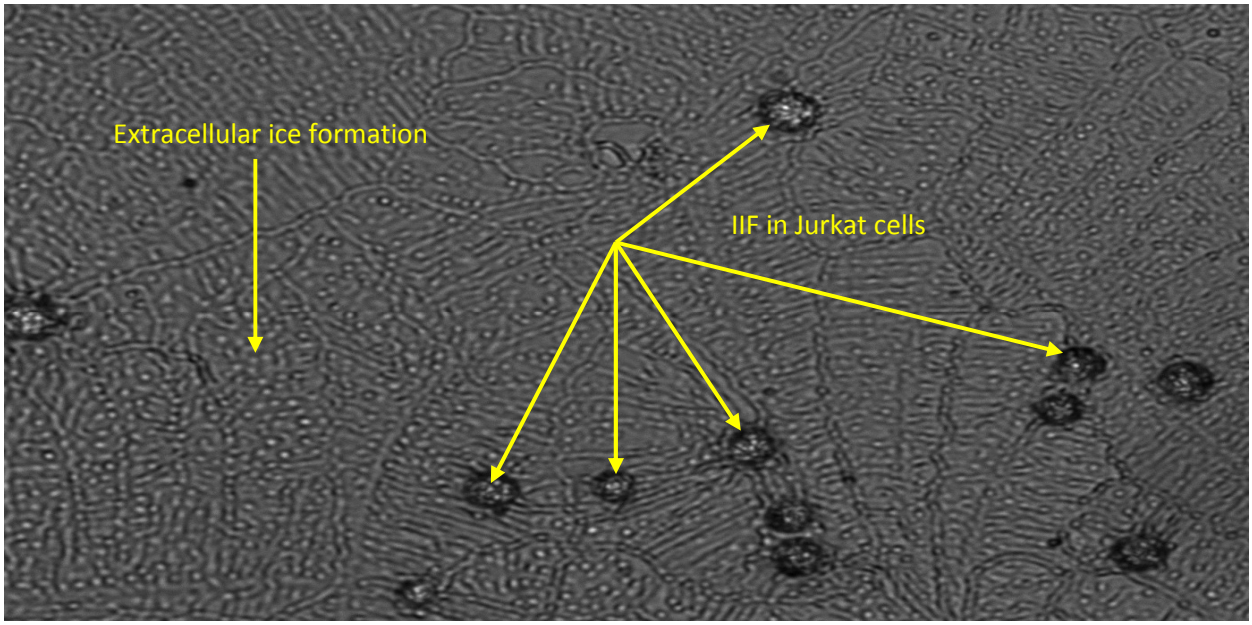

Figure 5.8: IIF in Jurkat cells at -18 ^{o}C approximately.

At approximately -18 ^{o}C, the Jurkat cells underwent ~ 100% IIF through blackening. As anticipated, IIF followed extracellular ice formation.

5.4.3 Results

Table 5.4 Temperature vs PIIF for Jurkat Cells at 10 ^{o}C/min

Temperature (^{o}C)	Percentage IIF(PIIF)
-16.4	8.33
-16.5	16.67
-16.6	33.33
-17	50
-17.2	67
-17.5	83.33
-18	100

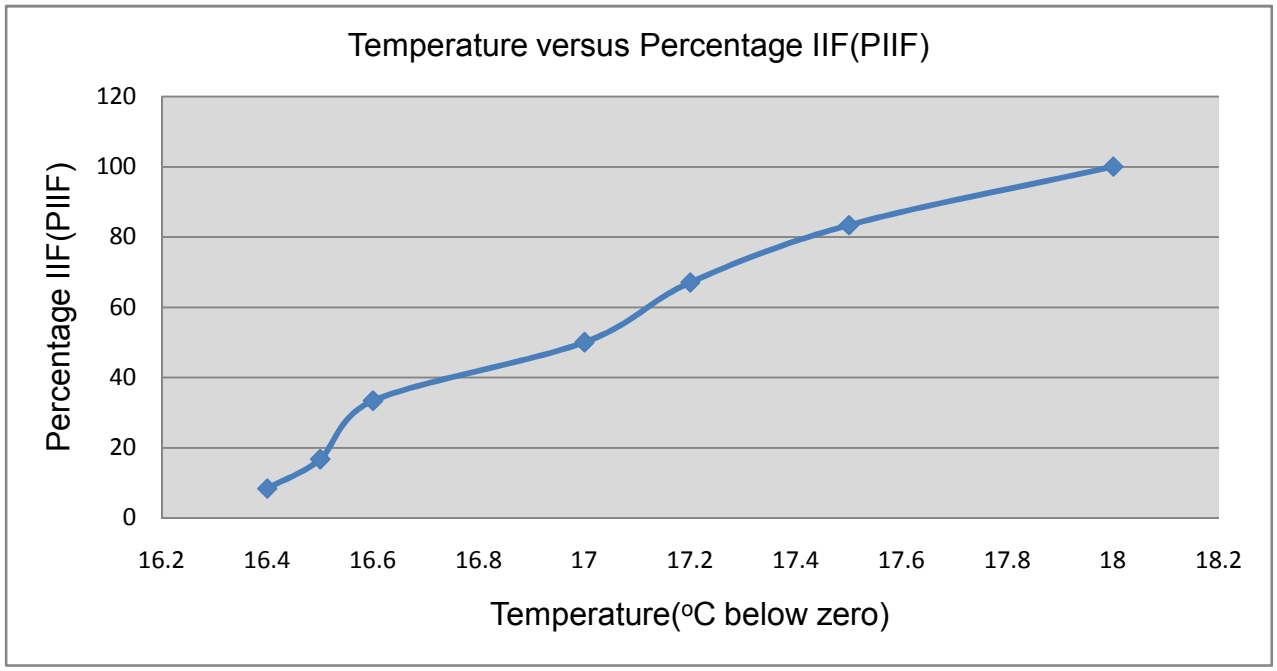

Figure 5.9: Variation of percentage IIF with decreasing temperature at a freezing rate of 10 °C/min.

5.5 Discussions and Conclusion

Reference permeability of cell membrane (L_{pg}) and activation energy of permeation (E_{Lp}), for Jurkat cells were calculated at freezing rate of 1 °C/min, which were found to be 0.04 μm / min-atm and 69.7 Kcal / mol. The optimal freezing rate was approximately evaluated to be 1.3 °C/min. Experiments were also performed on similar set of Jurkat cells at freezing rates of 5, 10, 15, 20, and 50 °C/min. While at 5 and 15 °C/min, the observations were inconclusive (data not reported), at 20 and 50 °C/min, events were too fast to be investigated using the cryomicroscope. However, conspicuous blackening of Jurkat cells was observed at 10 °C/min suggesting IIF at this rate. Thus, the calculated value for the optimal freezing rate, using the water transport data was probably validated. The results from this investigation were compared to those published earlier by Thirumala et al in 2007. Although the obtained value for L_{pg} bore a close relevance, the E_{Lp} value was very different from what they obtained (9.5 Kcal/mol).

The optimal freezing rate for Jurkat cells was calculated as 1.3 ^{o}C/min, and was different from the earlier published result (33.7 ^{o}C/min). It probably needs to be noted that cell shrinkage data was obtained at 20 ^{o}C/min by them, while in this work the cells underwent IIF at 10 ^{o}C/min.

From the two different studies, it could be interpreted that even though the cells belonged to the same species, they probably had other factors to account for. One might say it was difficult to compare biological systems which even belonged to the same species because their behavior tended to be functions of various factors such as their culturing conditions, ambient conditions, and the method of experiments. It might hence be noted that the technique used for evaluation of freezing response of these cells was Cryomicroscopy, while the technique used by Thirumala et al in 2007 was Differential Scanning Calorimetry.

6. Freezing Response of HeLa Cells

6.1 Background

A HeLa cell is an immortal cell line used in medical research that is derived from cervical cancer cells. It is said that the cervical cancer cells were obtained from one Ms. Henrietta Lacks who died of cervical cancer in 1951(Rebecca 2001). Hence, the name HeLa has been derived from the first two letters of Ms Lacks' first and last names. HeLa cells are termed as immortal because they can proliferate extremely rapidly, even when compared to other cancer cells. These cells have been extremely useful in cancer research since 1960s. They have been useful in understanding the differences between cancer cells and normal cells. In the present work, attempts have been made to understand the freezing response of HeLa cells at slow and fast freezing rates in order to obtain an optimal freezing rate that might aid future researchers in developing a protocol for cryosurgery.

6.2 Sample Preparation

HeLa cells were maintained in 25 cm^2 flasks (BD Falcon, Franklin Lakes, NJ) with 5 ml of Dulbecco's Modified Eagle's medium-reduced serum (DMEM-RS) supplemented with 3% fetal bovine serum (FBS) and incubated at 37 ^oC in a humidified atmosphere containing 5% CO_2. Hela cells were plated at a density of 80,000 cells per cm^2 in 12 well cultured plates (BD Falcon, Franklin Lakes, NJ) were allowed to adhere and grow for 24 h prior to trypsinization (0.25% Trypsin. In order to prepare the cells for experiments, the following steps were followed:

1. Aspiration of media from flask to waste
2. Addition of 5 ml of 1X Dulbecco's Phosphate Buffered Saline (DPBS) solution and swiveling in flask.

3. Addition of 5 ml of Trypsin and waiting for 10 minutes for HeLa cells to come off from the dish at room temperature. The flask was gently rocked periodically and observed under the microscope to make sure that the cells were detaching.
4. Addition of 5 ml of DMEM-RS + 3% FBS in order to stop Trypsin action.
5. Transfer of suspension to a 50ml centrifuge tube.
6. Spin down of cells at 2400 rpm for 5 min using Eppendorf Minispin Plus centrifuge.
7. Decant off supernatant
8. Re-suspension of cells in appropriate cell buffer (1X DPBS).

6.3 HeLa Experiments at 1 ^{o}C/min

Experiments on HeLa cells were started at 1 ^{o}C/min which seemingly was a "slow freezing rate" for most cells (Mazur 1963, Mazur 1970, Mazur 1977, Mazur 1984, and Toner et al 1990). It has also been seen that most biological systems undergo water transport at such a freezing rate (Mazur 1977). Hence it was interesting to see if the cells underwent dehydration at this freezing rate. Similar to Jurkat cells, the aim of this experiment was to evaluate the membrane permeability characteristics of a HeLa cell that might help in evaluation of an optimal freezing rate using the Generic Optimal Cooling Rate Equation (GOCRE) derived by Thirumala et al (Thirumala et al 2007).

6.3.1 Freezing Protocol at 1 ^{o}C/min

Table 6.1 Freezing Protocol for HeLa cells at 1 ^{o}C/min

Start temperature (^{o}C)	Rate (^{o}C/min)	End temperature (^{o}C)
20.3	10	4
4	1	-30

6.3.1.1 Description of the Protocol

The freezing protocol for HeLa cells was designed in a similar manner as done earlier for Jurkat cells in Chapter 5 of this thesis. The phase change temperature of the extracellular solution (1X DPBS) was known from the calculations used for Jurkat cells, and it was -0.6 ^{o}C approximately. The temperature of the sample was brought down from the room temperature which was 20.3 ^{o}C to 4^{o}C at a rate of 10 ^{o}C/min. Finally, the temperature of the sample was slowly reduced to -30 ^{o}C at a freezing rate of 1 ^{o}C/min with the intent of observing dehydration of the cell. Special attention was paid to observe changes in the shape of the cell in the vicinity of the phase change temperature of extracellular solution.

6.3.2 Observation

Below: A comparison of the HeLa cell's appearance at three different temperatures

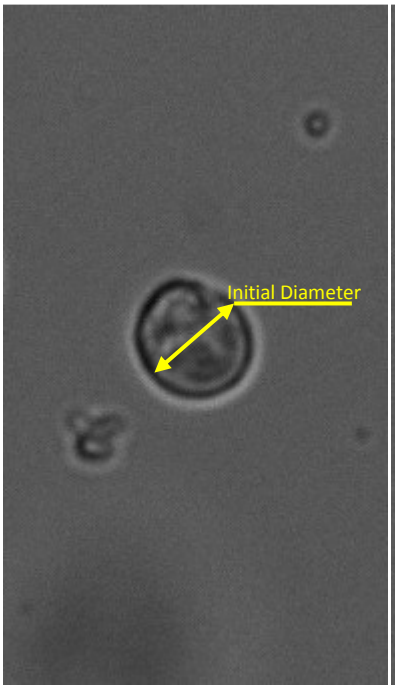

Figure 6.1
HeLa cell at 20.3 ^{o}C

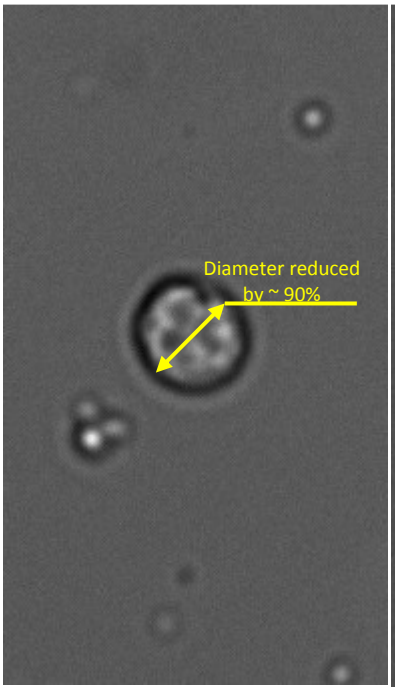

Figure 6.2
HeLa cell at -3 ^{o}C

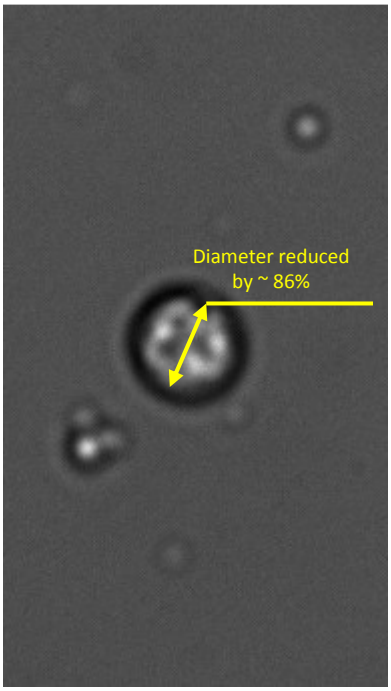

Figure 6.3
HeLa cell at -5 ^{o}C

Fig 6.1 showed the HeLa cell at a temperature of 20.3 ^{o}C. The image at room temperature was chosen in order to have an idea about the appearance, shape and size of the cell at room temperature. As could be seen from Fig 6.1, the cell appeared to be spherical and hence its diameter was noted on a linear scale. The diameter of HeLa cell was known from the results published by earlier researchers (15 +/- 1.5 µm) (Thirumala et al 2007). The diameter of the cell shown in Fig 6.2 was measured as a percentage of the diameter of the same cell measured in Fig 6.1. Fig 6.2, showed the cell being reduced to ~ 90% of its original diameter, which thus meant that it was reduced to ~ 73% of its original volume. Similarly, from Fig 6.3, it could be seen that the cell diameter was reduced to ~ 86% of the original diameter. Hence, the volume reduced to ~ 63% of the original volume.

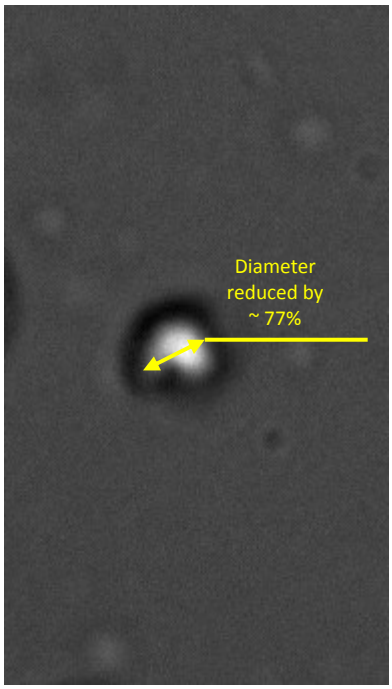

Figure 6.4

Left: HeLa cell at -10 ^{o}C.

On the left, Fig 6.4 showed the image of the Jurkat cell at -10 ^{o}C beyond which there was no significant change in the diameter of the cell. Approximately the cell shrunk to 45% of its original volume. The volume beyond which there was no further reduction could probably have been the inactive cell volume of HeLa cell. Work by Thirumala et al (Thirumala et al 2007) suggested that the inactive cell volume of HeLa cell was 0.45.

Thus, seemingly this result was in good agreement. It could now be imagined that the cell might have reduced in volume due to water transport.

6.3.3 Experimental Results

Table 6.2: Temperature vs Normalized Volume for HeLa Cells at 1 ^{o}C/min

Temperature (^{o}C)	Normalized volume (V/V_o)
-0.6	1
-1	0.96
-2	0.84
-3	0.73
-4	0.69
-5	0.65
-6	0.60
-7	0.56
-8	0.51
-9	0.45
-10	0.45

The HeLa cell seemingly started dehydrating somewhere between -0.6 ^{o}C and – 1^{o}C. There was no appreciable change in volume after ~ -9 ^{o}C. As mentioned in earlier literature (Mazur 1963, Mazur 1970, Mazur 1977, Mazur 1984, Toner et al 1990, Thirumala et al 2007), this was probably the inactive cell volume of HeLa cell that did not participate in exosmosis. The value of inactive cell volume (V_b) was an essential parameter that was useful in evaluating the membrane permeability characteristics (L_{pg} and E_{Lp}). The membrane permeability characteristics could hence be used to evaluate the optimal freezing rate using the well known Generic Optimal Cooling Rate Equation (GOCRE) derived by Thirumala and Devireddy in 2005.

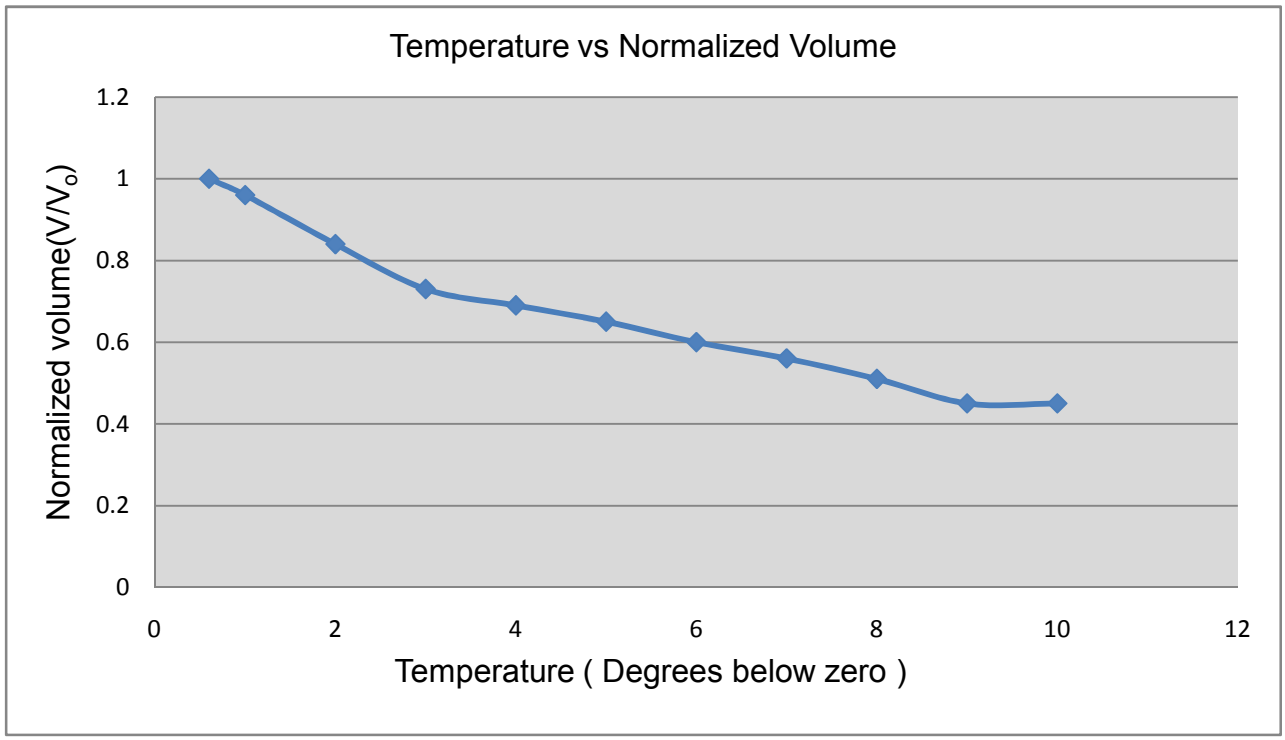

Figure 6.5: Variation of normalized volume with decreasing temperature

The normalized volume is the ratio of the volume at a particular temperature to the original volume. As mentioned before, apparently the cell did not shrink beyond a particular value of normalized volume, which was the inactive cell volume. The inactive cell volume for the HeLa cell was evaluated as 45% of the original cell volume.

6.3.4 Numerical Simulations

6.3.4.1 Water Transport Model

$$\frac{dV}{dT} = -\frac{L_P A R T}{v_w B}\left[\ln\frac{(V - V_b)}{(V - V_b) + v_w(n_s)} - \frac{\Delta H_f}{R}\left(\frac{1}{T_R} - \frac{1}{T}\right)\right] \ldots . (13)$$

$$L_P = L_{Pg} \exp\left[\frac{E_{Lp}}{R}\left(\frac{1}{T} - \frac{1}{T_R}\right)\right] \ldots . (14)$$

The above equations are collectively known as the water transport equations. The water transport equation represents the change in volume of a cell (during dehydration) as a function of temperature. As mentioned before, the right hand side of the equation represents the driving force as the difference between the chemical potentials of intracellular water and extracellular solution. In order to obtain L_{pg} and $E_{Lp,}$ it was necessary to have accurate information about V_b. The experimental result for inactive cell volume ($V_b \sim 0.45$) agreed with earlier obtained results (Thirumala et al 2007), as shown below.

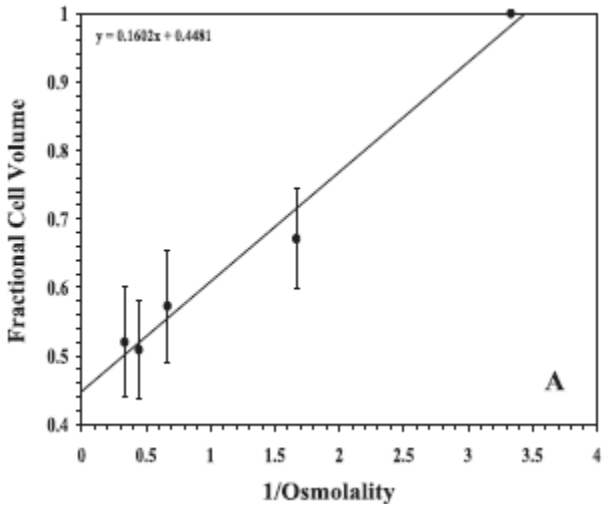

Figure 6.6 Y-intercept reveals inactive cell volume of HeLa cells (0.45) (Thirumala et al.2007)

The Boyle-Van't Hoff plot showed the changes in volume of HeLa cells when they were subjected to varying osmolalities (0.3, 0.6, 1.5, 2.25 and 3.00 Osm/kg) at temperature ~ 27 ^{o}C.

The biophysical parameters for water transport were hence estimated using a non linear regression algorithm as previously reported (Thirumala et al 2003, Thirumala et al 2005, Thirumala et al 2006).The experimentally measured water transport data at 1 ^{o}C/min for HeLa cells were compared to theoretically predicted curves (equations (13) and (14)).The biophysical parameters of water transport were iteratively adjusted until the chi squared variance, χ^2, was

minimized or a goodness-of-fit parameter, R^2, was maximized, (A value of 1 for R^2 would represent a perfect fit while a value of 0, a flawed fit.) using a gradient search method described in Bevington and Robison (Bevington and Robinson 1992). All reported parameters were obtained for an $R^2 > 0.95$.

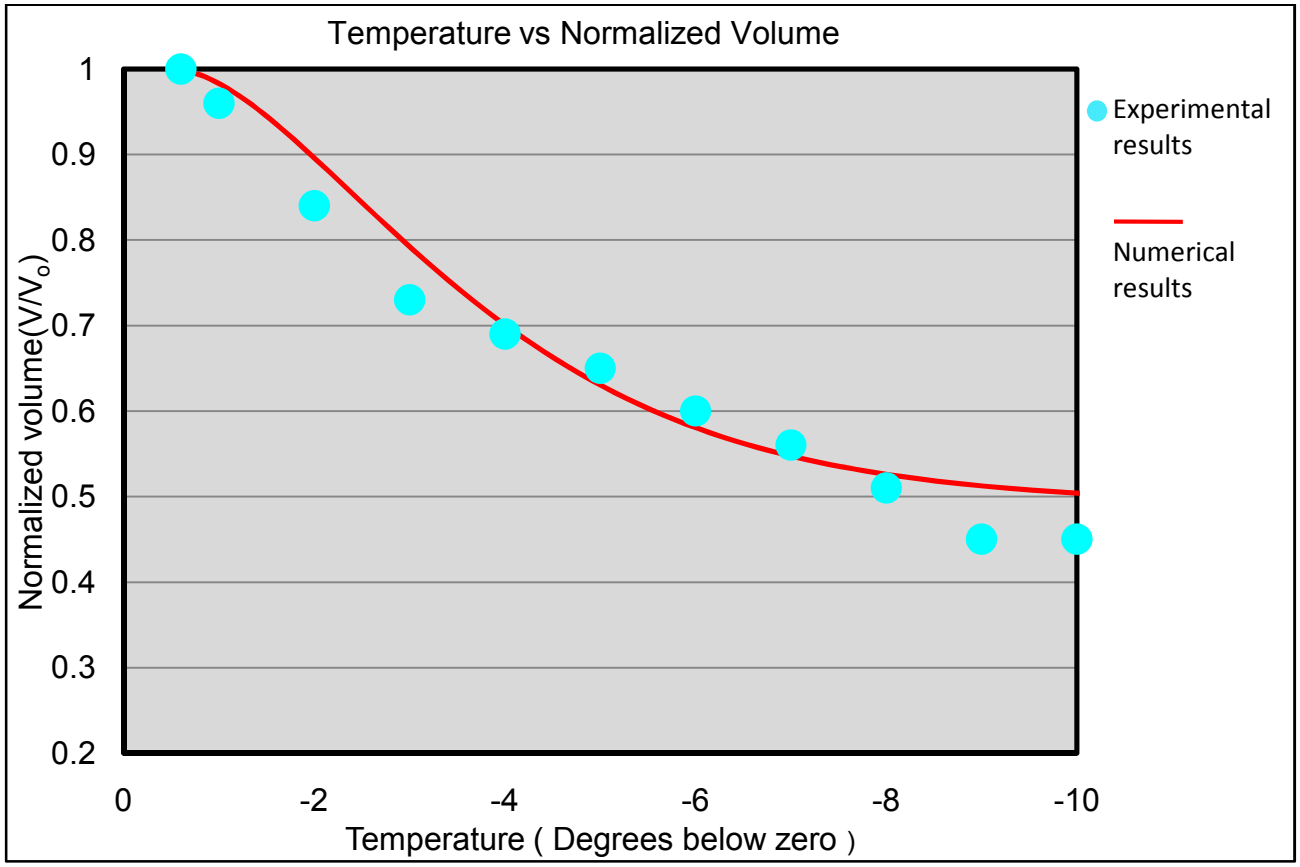

Figure 6.7: Numerical Simulation

The above plot shows a comparison between the experimentally obtained and the numerically simulated values of normalized volume of HeLa cells dehydrated using a freezing rate of 1 ^{o}C/min. The non-linear regression algorithm was used to fit the water transport equation into the experimentally obtained results of normalized volume at various temperatures. Using this model, the values of L_{pg} and E_{Lp} were obtained which were hence used to numerically simulate the volume shrinkage at various temperatures within the protocol.

6.4.3.2 Generic Optimal Cooling Rate Equation (GOCRE)

$$B_{optimal} = 1009.5 * \exp^{(-0.0546 * E_{Lp})} * (L_{pg}) * \frac{SA}{WV}$$

SA = surface area of the cell membrane

WV = Volume of water contained within the cell = $V_o - V_b$

L_{pg} = Reference permeability of cell membrane

E_{Lp} = Activation energy of permeation process

Using the above equation, the following results were obtained:

Cell	**L_{pg} (µm/min-atm)**	**E_{Lp} (Kcal/mole)**	**R^2**	**B_{opt} (^oC/min)**
HeLa	0.05	20.9	0.97	11.3

6.4 HeLa Experiments at 15 ^oC/min

From the earlier set of experiments on HeLa cells at a "slow cooling rate" of 1 ^oC/min, information about membrane permeability and hence the optimal cooling rate was obtained. As shown before, the optimal cooling rate was evaluated as 11.3 ^oC/min. It was thus decided to observe the freezing behavior of HeLa cells at higher freezing rates. A higher freezing rate of 15 ^oC/min was chosen and a protocol similar to Jurkat cells (Chapter 5) was designed in order to understand the reaction of these cells at a seemingly "fast freezing rate."

6.4.1 Freezing Protocol at 15 ^{o}C/min

Table 6.3 Freezing Protocol for HeLa Cells at 15 ^{o}C/min

Start temperature (^{o}C)	Rate (^{o}C/min)	End temperature (^{o}C)
19.5	15	4
4	1	-2.6
-2.6	1	-1.6
-1.6	15	-30
-30	15	20

6.4.1.1 Description of the Protocol

HeLa cells were suspended in 1X DPBS solution (isotonic for them). The freezing point of the extracellular solution (1X DPBS) was evaluated as ~ -0.6 ^{o}C, using calculations shown in equation (27). Hence the temperature of the suspension was brought down from the room temperature i.e. 19.5 ^{o}C to 4 ^{o}C at a rate of 15 ^{o}C/min in order to speed up the process. As mentioned before, this step was introduced only to speed up the process and it did not have any significant influence on the outcome of the experiment. The temperature was decreased till -2.6 ^{o}C (2 degrees below 1X DPBS's phase change temperature). System was held at this temperature in to ensure extracellular ice formation. Hence, the temperature was slightly elevated to -1.6 ^{o}C and finally it was frozen between this temperature and -30 ^{o}C at the desired freezing rate i.e.15 ^{o}C/min. It was learnt from previous literatures (Toner et al 1990, and Toner 1993) that extracellular ice through some yet unknown mechanism transformed supercooled intracellular water into ice. Thus the phase change temperature of the extracellular solution (1X DPBS) was an important parameter used in designing this protocol.

6.4.2 Observation

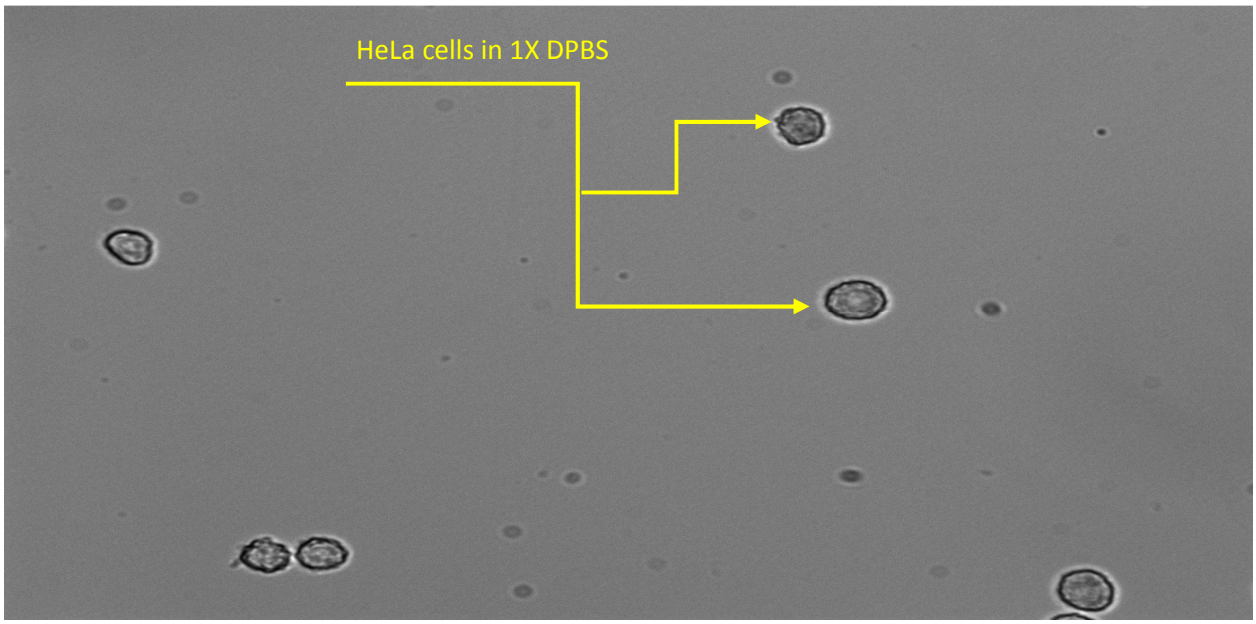

Figure 6.8: The above image shows HeLa cells in 1X DPBS solution at a room temperature of 19.5 ^{o}C. This image was reported in order to learn about the appearance of HeLa cells at the beginning of the freezing experiment.

At the room temperature, as could be seen from above, 6 HeLa cells were focused on. The extracellular solution used in this experiment was the same as before, 1X DPBS. Since it was learnt from the previous set of experiments on HeLa cells that they had an optimal freezing rate of 11.3 ^{o}C/min, it was now interesting to see how they behaved at a higher freezing rate of 15 ^{o}C/min. Hence, there was anticipation that IIF could be seen in HeLa cells at this rate and the protocol, as mentioned before, was decided accordingly. It was learnt from the earlier IIF experiments on Pacific Oyster embryos and Jurkat cells that IIF followed extracellular ice formation. Hence, an important parameter was the phase change temperature of the extracellular solution (1X DPBS) which was theoretically determined as ~ -0.6 ^{o}C. It was now to be seen if the HeLa cells within the field of view underwent intracellular ice formation (IIF) in the vicinity of this temperature.

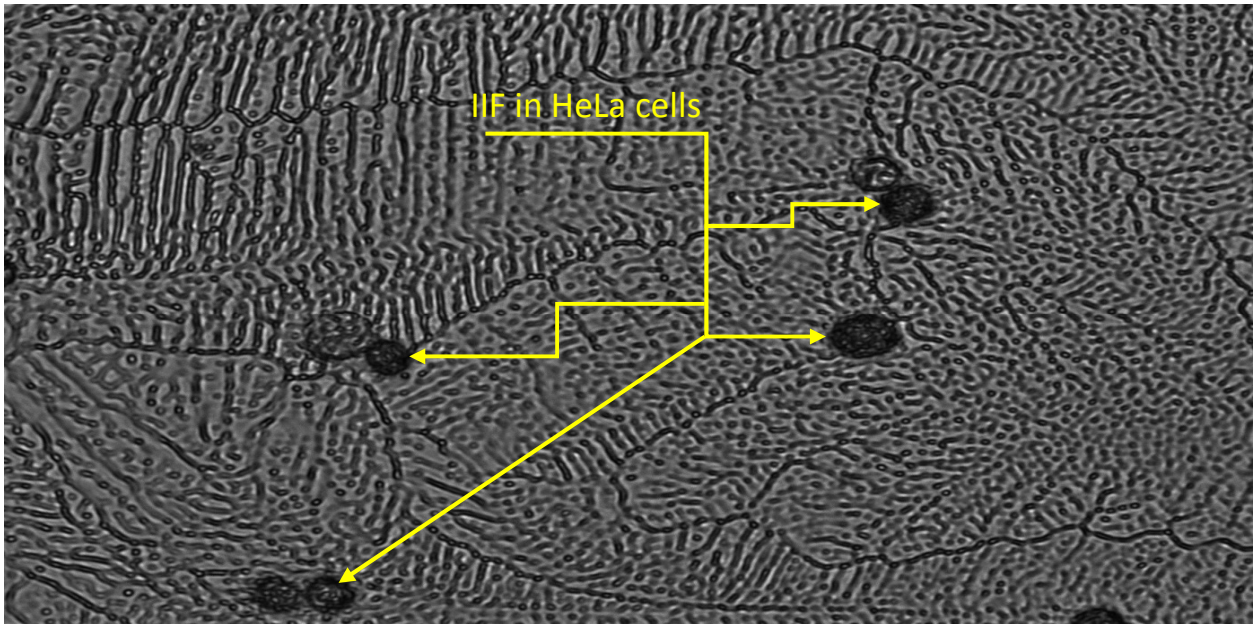

Figure 6.9: Above image shows IIF in HeLa cells at ~ -12 ^{o}C. IIF was noticed through darkening of cells. As seen before (Chapters 4 and 5), IIF followed after the formation of extracellular ice.

6.4.3 Results

Table 6.4 Temperature vs PIIF for HeLa Cells at 15 ^{o}C/min

Temperature (^{o}C)	Percentage IIF(PIIF)
-2.5	18.75
-4.3	25
-6	62.5
-8	87.5
-11.5	93.75

The results shown above were obtained from two consecutive sets of experiments at a freezing rate of 15 ^{o}C/min and using the same protocol. Percentage IIF was evaluated as the ratio of the total number of cells that underwent IIF to the total number of cells present within the field

of view during the experiment. Hence, two consecutive identical runs revealed that approximately 15 out of 16 cells underwent IIF at ~ -12 ^{o}C.

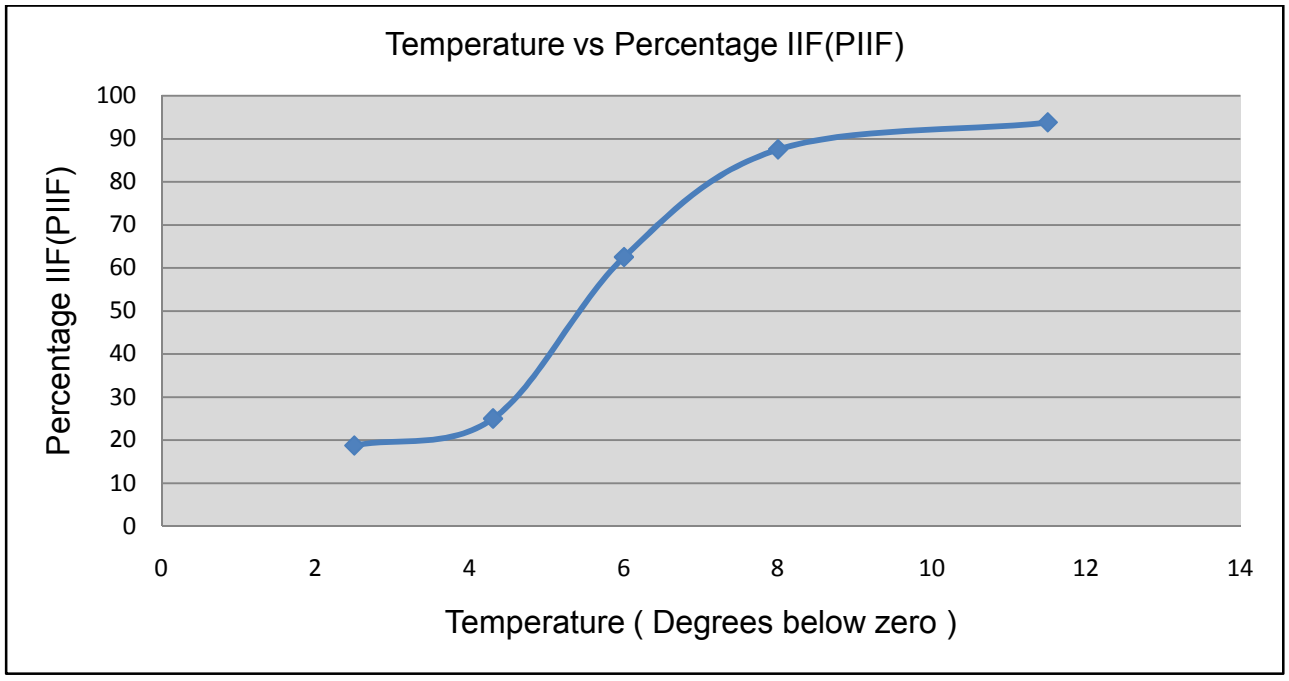

Figure 6.10: Variation of percentage IIF with decreasing temperature

As mentioned earlier, it was revealed that apparently 15 ^{o}C/min was a "fast freezing rate" for HeLa cells that caused IIF among them. Two consecutive experimental runs revealed that approximately 94% of the HeLa cells underwent IIF at this freezing rate. The experimental results obtained for HeLa cells probably validated the result from the water transport experiments on them at 1 ^{o}C/min. From the data obtained through those experiments and subsequent simulation, the optimal freezing rate for HeLa cells was evaluated as 11.3 ^{o}C/min.

Following this, it was now decided to perform another set of freezing experiments on HeLa cells at a higher freezing rate. Hence, a freezing rate of 20 ^{o}C/min was chosen. It would have been interesting to observe if IIF was also conspicuous at this freezing rate. Hence, the final set of experiments were performed on HeLa cells using a freezing rate of 20 ^{o}C/min.

6.5 Hela Experiments at 20 ^{o}C/min

6.5.1 Freezing Protocol at 20 ^{o}C/min

Table 6.5 Freezing Protocol for HeLa Cells at 20 ^{o}C/min

Start temperature (^{o}C)	Rate (^{o}C/min)	End temperature (^{o}C)
20	20	4
4	1	-2.6
-2.6	1	-1.6
-1.6	20	-30
-30	20	20

6.5.1.1 Description of the Protocol

After viewing IIF in HeLa cells at a freezing rate of 15 ^{o}C/min, another set of experiments was performed at a freezing rate of 20 ^{o}C/min using the same protocol as before.

6.5.2 Observation

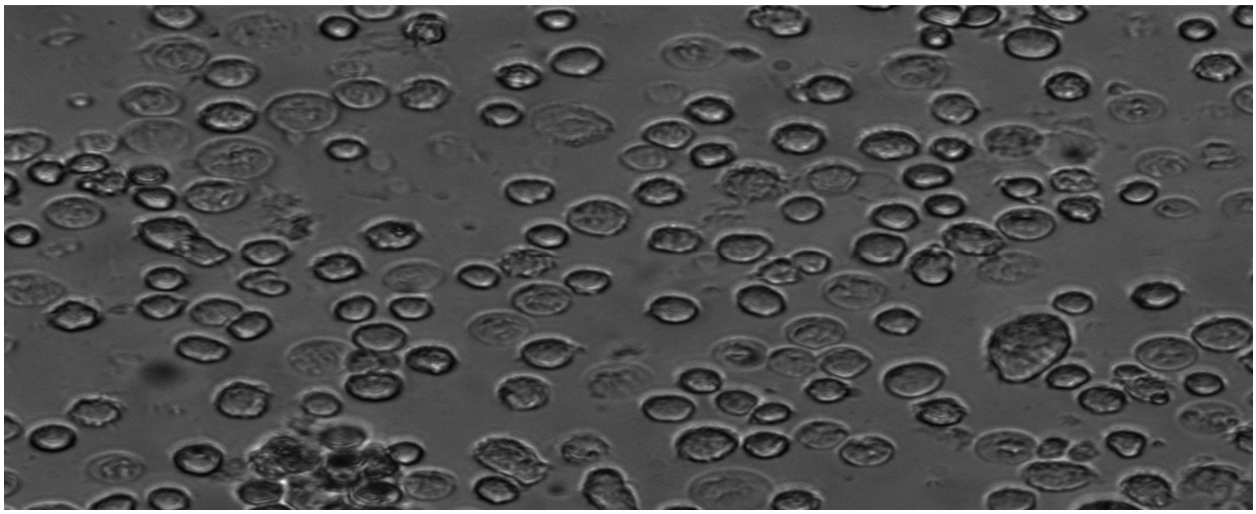

Figure 6.11: HeLa cells in 1X DPBS before the freezing process started

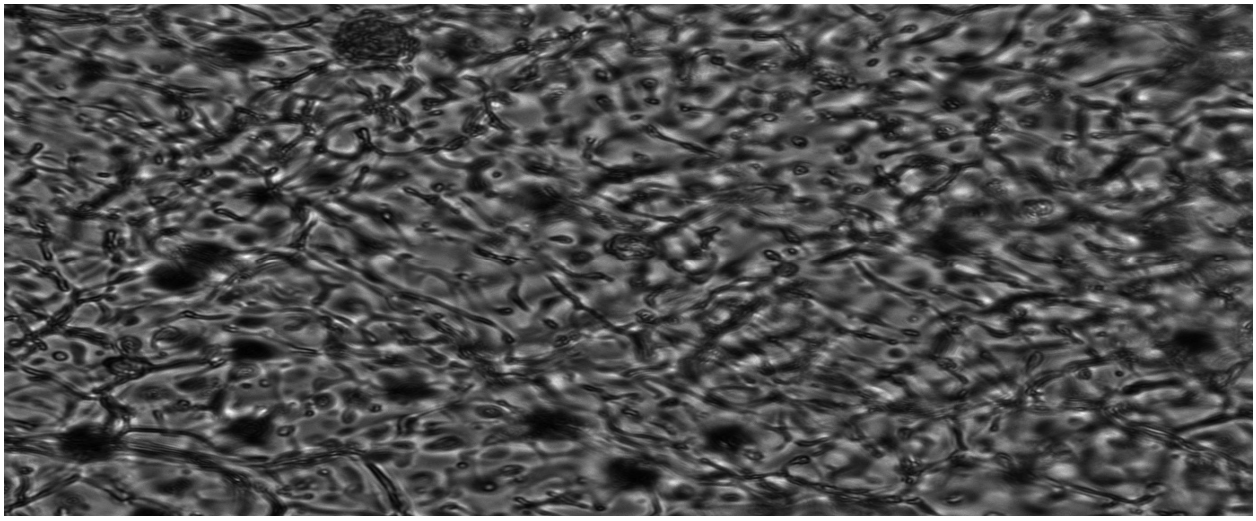

Fig 6.12: HeLa cells showing IIF at a freezing rate of 20 ^{o}C/min and at ~ -19 ^{o}C

6.5.3 Results

Table 6.6 Temperature vs PIIF for HeLa Cells at 20 ^{o}C/min

Temperature (^{o}C)	Percentage IIF(PIIF)
-2	3.25
-4	9
-6.9	15.25
-7.8	22.25
-9.6	30
-11.6	39
-13.45	48.5
-15.35	58.5
-17.3	69.5
-19.2	81

Maximum IIF observed through blackening was 81% at -19.2 ^{o}C

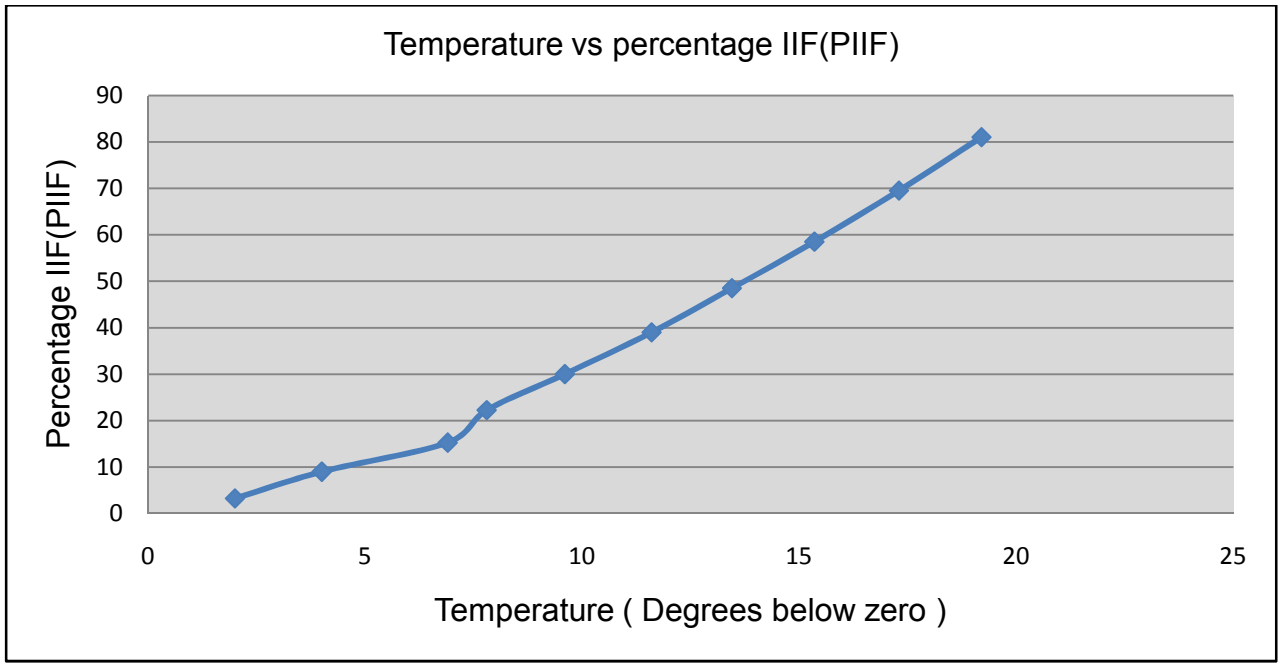

Figure 6.13: Variation of percentage IIF with decreasing temperature at a freezing rate of 20 ^{o}C/min.

6.6 Discussions and Conclusion

Reference permeability of cell membrane (L_{pg}) and activation energy of permeation (E_{Lp}), for HeLa cells were calculated at freezing rate of 1 ^{o}C/min, which were found to be 0.05 μm / min-atm and 20.9 Kcal / mol. The optimal freezing rate was approximately evaluated to be 11.3 ^{o}C/min. Freezing experiments on HeLa cells were also carried out at 10 ^{o}C/min, 15 ^{o}C/min, 20 ^{o}C/min, 30 ^{o}C/min, and 50 ^{o}C/min. While IIF was seen through blackening of cells at 15 ^{o}C/min and 20 ^{o}C/min, there was no conclusive observation at 10 ^{o}C/min (data not reported). In addition, IIF at higher freezing rates was extremely rapid and images could not be accurately captured by the camera. The results from this investigation were compared to those published earlier by Thirumala et al in 2007. Although the obtained value for L_{pg} bore a close relevance to their result (0.08 μm / min-atm), the E_{Lp} value varied from their data (10.9 Kcal/mol). In this work, the optimal freezing rate for HeLa cells was calculated as 11.3 ^{o}C/min, and was different

from the earlier published result (30.6 ^{o}C/min). It probably needs to be noted that cell shrinkage data was obtained at 20 ^{o}C/min by them, while in this work the cells underwent IIF at 15 ^{o}C/min.

The diversity in the nature of the results would probably make researchers wonder about other factors that might make a certain cell type behave differently to similar freezing conditions. It might be believed that some cells had a range of optimal freezing rates and seemingly they varied under different conditions. The freezing response on a given cell type might also be influenced by its culturing conditions, method of experiment or ambient conditions. It would be worth mentioning here that the technique used for analysis of freezing response of the chosen cells in this work was cryomicroscopy while it was Differential Scanning Calorimetry in Thirumala et al.'s work.

7. Conclusions and Future Work

7.1 Conclusions

Freezing experiments were performed on three different types of cells. As mentioned before, the three different cell types used were Pacific oyster embryo, Jurkat and HeLa. On a primary basis, research on these cell types was done in order to support ongoing research activities at the Bioengineering Laboratory in the Department of Mechanical Engineering at Louisiana State University, Baton Rouge. On a secondary basis, this research aimed at providing useful information to future researchers who intended to develop successful protocols for cryopreservation and cryosurgery. One important goal of this work was to evaluate the optimal freezing rate for the cell types. Although an optimal freezing rate for Jurkat and HeLa cells could be evaluated, it could not be evaluated for Pacific Oyster embryos because research activities were limited due to unavailability of the embryos through most part of the season.

The optimal freezing rate is a measure of the freezing rate at which a given cell type shows maximum viability. One way of evaluating optimal freezing rate is by performing freezing experiments on cells at seemingly "slow freezing rates" in order to obtain the membrane permeability characteristics (reference permeability of cell membrane and activation energy of permeation). Membrane permeability characteristics could be used in Generic Optimal Cooling Rate Equation (GOCRE) to obtain an optimal freezing rate. In this work, this method was used to evaluate the optimal freezing rate of Jurkat and HeLa cells. Hence, the important parameters evaluated in this work were reference permeability of cell membrane (0.04 μm/min-atm for Jurkat cell and 0.05 μm/min-atm for HeLa cell) and activation energy of permeation (69.7 Kcal/mol for Jurkat cell and 20.9 Kcal/mol for HeLa cell). The evaluated optimal freezing rates for Jurkat and HeLa cells were 1.3 ^{o}C/min and 11.3 ^{o}C/min respectively.

Useful information could also be obtained by performing freezing experiments at seemingly "fast freezing rates." Such experiments would aim at identifying the freezing rates at which intracellular ice formation (IIF) was evident. It is known that IIF is generally lethal to cell survival. Thus, information about such freezing rates that trigger IIF in a given cell type may provide valuable information to researchers working on developing protocols for cryopreservation or cryosurgery. In this work, IIF through darkening of cells was observed in Jurkat cells at 10 ^{o}C/min, in HeLa cells at 15 and 20 ^{o}C/min, and in Pacific Oyster embryos at 5 and 10 ^{o}C/min.

It was learnt from earlier literatures that all biological systems showed similar responses to freezing. However, the two biophysical phenomena, water transport and intracellular ice formation (IIF) might be observed under varying conditions among different biological systems. While a given freezing rate could trigger IIF in a particular biological cell, it might only lead to dehydration in another type of cell. For example, in this work, the Pacific Oyster embryos appeared to undergo IIF at a much lower freezing rate (5 ^{o}C/min) than Jurkat and HeLa cells. It was probably thus worthwhile to briefly investigate the biological differences among the three biological systems chosen for this work.

One possible reason for Pacific Oyster (Crassostrea gigas) embryos to have a sufficiently low IIF causing freezing rate could be attributed to their large size. The diameter of the Pacific Oyster embryos was 50 μm approximately. It is learnt that ice formation is primarily a statistical phenomenon and thus probability of ice formation is proportional to the surface area on which it takes place. It would hence probably follow that Pacific Oyster embryos being larger in size than Jurkat and HeLa cells and under same experimental conditions would demonstrate a lower IIF freezing rate. Another important biological difference between Pacific Oyster embryos and other

cells used in this research was the fact that Pacific Oyster embryos were multicellular while Jurkat and HeLa cells were unicellular. Probably this would also indicate that the quantity of cytosol in a multicellular embryo was more than in a unicellular system.

Jurkat cells are immortalized cell lines derived from human T cell lymphocytes. The diameter of Jurkat cell was evaluated as 12 μm approximately (Thirumala et al 2007). Jurkat cells are used to study T cell leukemia, T cell signaling and the expression of various chemokine receptors susceptible to viral entry. T cell lymphocytes are a group of white blood cells that play an important role in cell mediated immunity where T cells react to antigens with release of chemicals called as cytokines. T cells are different from other cells through their T cell receptor which is probably used for recognizing antigens. T cells originate in hematopoietic stem cells in bone marrow and thus develop in thymus, and hence the abbreviation 'T' stands for thymus. The growth of Jurkat cells is promoted by a factor secreted by the cell line of Squamous Cell Carcinoma of head and neck. Squamous Cell Carcinoma is a malignant tumor of Squamous Epithelium (Pawelec et al, 1982).

As mentioned before, HeLa cells are immortalized cell lines derived from cervical cancer cells of Henrietta Lacks (1920-1951) and hence the abbreviation followed from there. The diameter of HeLa cell was evaluated as 15 μm approximately (Thirumala et al 2007). The physiology of HeLa cells has been studied in thin sections with the electron microscope and several unusual features have been reported (Epstein 1961). There have been reports of HeLa cells being flattish and irregularly rounded, with large oval or kidney shaped nuclei and prominent nucleoli. Various sized oval or rounded profiles of smooth surfaced vesicles of endoplasmic reticulum were found to be scattered all over the cytoplasm. In some cells, chains of such vesicles extended inwards from the cell membrane at the base of microvilli (microscopic

cellular membrane protrusions that increased surface area of cells and were probably involved in a wide variety of functions such as absorption, secretion, cellular adhesion and conversion of mechanical stimulus to chemical activity). It was also reported that large areas of cytoplasm near the nucleus were filled with swarms of small smooth vesicles, and were associated with randomly disposed piles of small smooth surfaced cisternae. Some of the other observations included infrequent rough surfaces on endoplasmic reticulum, sparsely scattered mitochondria throughout the cell, and presence of large dense lipid bodies or digestive vacuoles. It was also observed that a small portion of cells had considerable areas of cytoplasm devoid of organelles, but occupied by unknown uniform fuzzy material (Epstein 1961).

Although it is difficult to directly relate these biological aspects of the cells to their freezing response, it could probably be imagined that their biological differences might also have a role to play. However, as mentioned before, the size of the cell could definitely be a governing factor as it determines the volume of water contained. The greater the volume of water contained within the cell, the lesser should be the freezing rate in order to allow it to escape through the semi-permeable membrane at an osmotic pressure gradient. It is hence to be seen how the evaluated membrane permeability characteristics from this work compare with other literatures.

To the best of our knowledge, none other than Thirumala et al in 2007 had evaluated the membrane permeability characteristics and optimal freezing rate for Jurkat and HeLa cells. As mentioned before, results from this work were compared to their work. Although the reference permeabilities for both Jurkat and HeLa cells bore close relevance, there were differences in the values obtained for activation energy and optimal freezing rate.

The discrepancies could have been resulted from various factors such as cell culturing conditions, time and methods of experiments. It would be noted that cryomicroscopy was the

sole technique used in this work, while Differential Scanning Calorimetry was used in the work by Thirumala et al in 2007.

7.2 Future Work

The need to research on Pacific Oyster embryos was based on their increasing demand and unavailability during most part of the year. Fast freezing rate experiments on oyster embryos led to the observation that they probably could not be cryopreserved even at a freezing rate of 5 ^{o}C/min. Future researchers might need to experiment on oyster embryos using slower freezing rates in order to develop an optimal freezing rate. The experimental results using "fast freezing rates" would also require being curve fit on the 'IIF equation (equations 17 and 18) in order to obtain κ_o (thermodynamic parameter) and Ω_o (kinetic parameter). These parameters would help in numerically evaluating the probability of intracellular ice formation (PIIF) between a given seeding temperature and a subzero temperature.

Research on Jurkat and HeLa cells was also based on the need to learn more about their response to a freezing stress which might help in devising either a cryopreservation or a cryosurgical protocol. Knowledge of an optimal freezing rate would probably indicate towards the destruction of such cells beyond that freezing rate. In order to obtain the optimal freezing rate, the generic optimal cooling rate equation (GOCRE) (Thirumala and Devireddy 2005) was used. However, there was considerable discrepancy in the values of optimal freezing rates evaluated in this work and by Thirumala et al in 2007. It would be worth mentioning that the techniques used in the evaluation of freezing response were Cryomicroscopy in this work and Differential Scanning Calorimetry by Thirumala et al. Future work might indicate towards repeating the experiments under similar conditions and using both the techniques, in order to evaluate the optimal freezing rates.

It has been seen that different cells behave differently to a given freezing stress. While a certain freezing rate triggers dehydration in a particular cell type, it may also lead to intracellular ice formation in another cell type. Hence, evaluation of freezing response of various cells becomes a far more challenging task than can ever be imagined. One major issue is to understand the effect of IIF on cell death. It has been proposed that cooling rates resulting in 50% IIF within the cells result in only 50% survival (Toner 1993). It is a well known fact that the maximum survival after a freeze-thaw protocol occurs if the freezing is slow enough to avoid IIF and fast enough to minimize the damaging effects of water transport. However, as mentioned before, different cells have shown extremely varied optimal freezing rates compatible with their maximum survival rate.

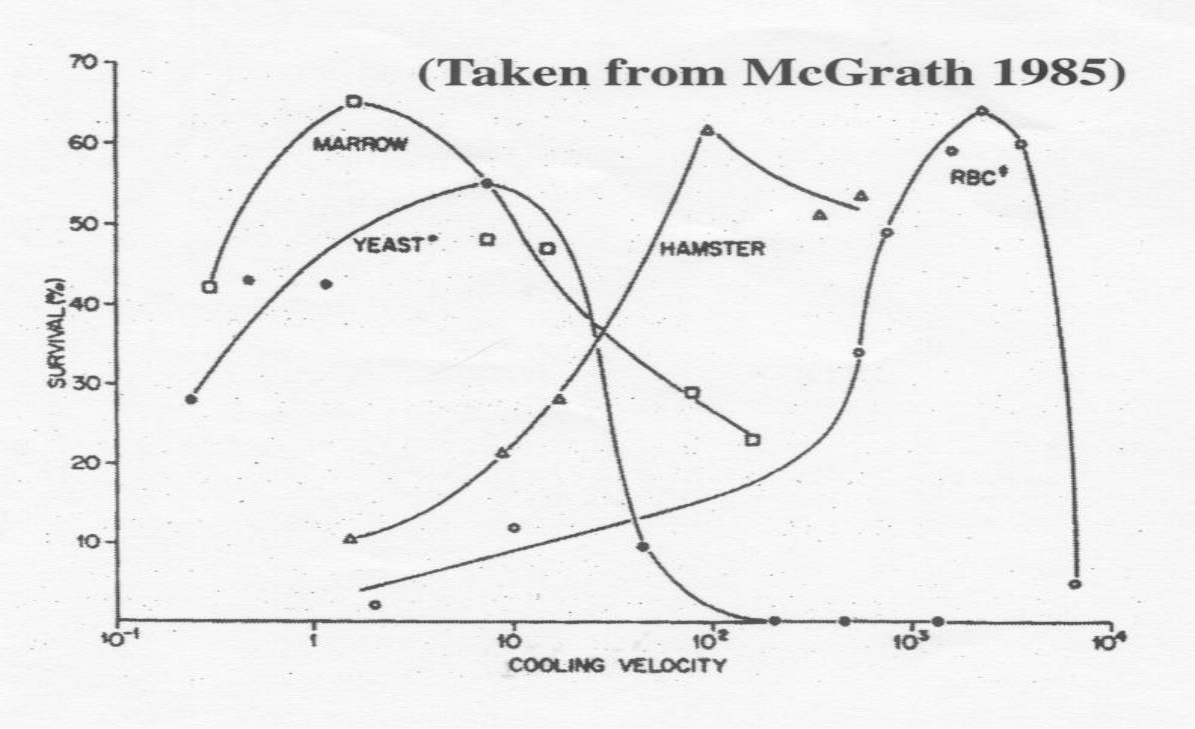

Fig 7.1: Variation of percentage survival of different cell types with various cooling rates.

It could be seen that while Red Blood Corpuscles (RBC) showed maximum survival in excess of 1000 ^{o}C/min, marrow cells showed maximum survival at a freezing rate close to 1

^{o}C/min (McGrath 1985). It might be related that the optimal freezing rate of cells were also dependent on the two water transport parameters namely L_{pg} (reference permeability of cell membrane) and E_{Lp} (activation energy of permeation). One might hence want to learn how these two parameters varied for different cell types. Some examples are as follows (Thirumala 2004):

Table 7.1 Variation in Membrane Permeability Characteristics of Certain Cell Types

Cell type	L_{pg}(μm $min^{-1}atm^{-1}$)	E_{Lp}(Kcal mol^{-1})
Human hepatocytes	0.97	51.6
Lymphocytes	0.10	15.5
Hematopoietic stem cells	0.064	69

The fact that determination of these parameters and subsequently the optimal freezing rate for millions of varieties of cells is an extremely challenging task may make future researchers to imagine about newer methods to understand the freezing response of cells. It would hence be wondered that if biological systems could be classified based on certain characteristics that made evaluation of the optimal freezing rates a much simpler task.

References

Anderson, M. D., "*Through the microscope: science probes an unseen world*," The Natural History Press, Garden City, New York, 1965

Balasubramanian, S., Bischof, J., Hubel, A., "*Water transport and IIF parameters for a connective tissue equivalent*," Cryobiology, 2005, 52, p. 62-73

Barmak, K., Harhaj, E., Grant, C., Alefantis, T., Wigdahl, B., "*Human T cell leukemia virus type I-induced disease: pathways to cancer and neurodegeneration*," Virology, 2003, 308, p. 1-12

Bernard, A., and Fuller, B. J., "*Cryopreservation of human oocytes: a review of current problems and perspectives*," Human Reproduction Update, 1996, 2(3), p. 193-207

Bevington, P. R., and Robinson, D. K., "*Data reduction and error analysis for the physical sciences, volume 2, New York: McGraw-Hill, 1992*"

Cooper, I. S., and Lee, A. S., "*Cryostatic congelation: a system for producing a limited, controlled region of cooling or freezing of biological systems*," The Journal of Nervous and Mental Disease, 1961, 133, p. 259-263

Cooper, I. S., "*Cryogenic surgery. A new method of destruction or extirpation of benign or malignant tissues*," The New England Journal of Medicine, 1963, 268, p. 743-749

Cosman, M., D., Toner, M., Kandel, J., Cravalho, E, G., "*An integrated cryomicroscopy system*," Cryo-Letters, 1989, 10, p. 17-38

Davson, H., and Danielli, J. F., "*The permeability of natural membranes*," Cambridge, The University Press, 2nd edition," 1952

Day, S. H., Nicoll-Griffith, D. A., Silva, J. M., "*Cryopreservation of rat and human liver slices by rapid freezing*," Cryobiology, 1999, 38, p. 154-159

Devireddy, R.V., Raha, D. and Bischof, J. C., "*Measurement of water transport during freezing in cell suspensions using a differential scanning calorimeter*," Cryobiology, 1998, 36, p. 124-155

Devireddy, R. V., and Bischof, J. C., "*Measurement of water transport during freezing in mammalian liver tissue-part II: The use of differential scanning calorimetry*," ASME Journal of Biomechanical Engineering, 1998, 120, p. 559-569

Devireddy, R. V., Smith, D. J., Bischof, J. C., "*Mass transfer during freezing in rat prostate tumor tissue*," American Institute of Chemical Engineers Journal, 1999, 45(3), p. 639-654

Devireddy, R. V., Swanlund, D. J., Roberts, K. P., Bischof, J. C., "*Sub-zero water permeability parameters of mouse spermatozoa in the presence of extracellular ice and cryoprotective agents*," Biology of Reproduction, 1999, 61(3), p. 764-775

Devireddy, R. V., Swanlund, D. J., Roberts, K. P., Pryor, J. L., Bischof, J. C., "*The effect of extracellular ice and cryoprotective agents on the water permeability parameters of human sperm plasma membrane during freezing*," Human Reproduction, 2000, 15, p. 1125-1135

Devireddy, R. V., Coad, J., Bischof, J., "*Microscopic and calorimetric assessment of freezing processes in uterine fibroid tumor tissue*," Cryobiology, 2001, 42(4), p.225-243

Devireddy, R. V., Olin, T., Vincente, W.,Troedsson, M. H. T., Bischof, J. C., Roberts, K. P., "*Cryopreservation of equine spermatozoa: Optimal cooling rates in the presence and absence of cryoprotective agents*," Biology of Reproduction, 2002, 66, p. 222-231

Diller, K. R., Cravalho, E. G., "A *cryomicroscope for the study of freezing and thawing processes in biological cells*," Cryobiology, 1970, 7, p. 191-199

Diller, K. R., "*Quantitative low temperature optical microscopy of biological systems*," Journal of Microscopy, 1982, 126, p. 9-28

Diller, K. R., "*Bioheat and mass transfer as viewed through microscope*," Journal of Biomechanical engineering, 2005, 127, p. 67-84

Dong, Q., Eudeline, B., Huang, C., Allen, S. K. Jr., Tiersch, T. R., "*Commercial scale sperm cryopreservation of diploid and tetraploid Pacific Oysters, Crassostrea gigas*," Cryobiology, 2005, 50(1), p. 1-16

Dong, Q., Huang, C., Eudeline, B., Tiersch, T. R., "*Systematic factor optimization for cryopreservation of shipped sperm samples of diploid Pacific Oysters, Crassostrea gigas*, Cryobiology, 2005, 51(2), p. 176-197

Dong, Q., Huang, C., Eudeline, B., Allen, S. K. Jr., Tiersch, T. R., "*Systematic factor optimization for sperm cryopreservation of tetraploid Pacific Oysters, Crassostrea gigas*," Theriogenology, 2006, 66(2), p. 387-403

Dong, Q., Huang, C., Tiersch, T. R., "*Control of sperm concentration is necessary for standardization of sperm cryopreservation in aquatic species: evidence from sperm agglutination in oysters*," Cryobiology, 2007, 54(1), p. 87-98

Epstein, M. A., "*Some unusual features of fine structure observed in HeLa cells*," The Journal of Biophysical and Biochemical Cytology, 1961, 10, p. 153-162

Gage, A. A., "*Cryosurgery in the treatment of cancer*," Surgery Gynecology and Obstetrics, 1992, 174, p. 73-92

Gage, A. A., and Baust, J., "*Mechanisms of tissue injury in cryosurgery*," Cryobiology, 1998, 37, p. 171-186

Gwo, J. C., "*Cryopreservation of oyster (Crassostrea gigas) embryos*," Theriogenology, 1995, 43(7), p. 1163-1174

Hagedorn, M., Hsu, E., Pilatus, U., Wildt, D. E., Rall, W. F., Blackband, S. J., "*Magnetic resonance microscopy and spectroscopy reveal kinetics of cryoprotectant permeation in a multicompartmental biological system.*" In: Proceedings of the National Academy of Sciences, 1996, 93, p. 7454-7459

Harris, C. L., Toner, M., Cravalho, E.G., "*Cryopreservation of isolated hepatocytes: intracellular ice formation under various chemical and physical conditions*," Cryobiology, 1991, 28, p. 436-444

He, Y., Dong, Q., Tiersch, T., Devireddy, R. V., "*Variation in the membrane transport properties and predicted optimal rates of freezing for spermatozoa of diploid and tetraploid oyster, Crassostea gigas*," Biology of Reproduction, 2004. 70, p. 1428-1437

Hong, J., Rubinsky, B., "*Patterns of ice formation in normal and malignant breast tissue*," Cryobiology, 1994, 31(2), p. 109-120
Ishiguro, H., Rubinsky, B., "*Mechanical interaction between ice crystals and red blood cells during directional solidification*," Cryobiology, 1994, 31, p. 483-500

Levin, R. L., Cravalho, E. G., Huggins, C. G., "A membrane model describing the effect of temperature on water conductivity of erythrocyte membranes at subzero temperatures," Cryobiology, 1976, 13, p. 415-429

Lin, T. T., Chao, N. H., Tung, H. T., "*Factors affecting survival of cryopreserved oyster (Crassostrea gigas) embryos*," Cryobiology, 1999, 39(2), p. 192-196

Lin, T. T., Lung, K., "*IIF characteristics of oyster embryos and eggs determined by a feedback controlled directional cryomicroscope*," Cryobiology, 1995, 32, p. 566

Linkam Scientific Instruments Ltd, L.S.I., "*BCS 196 Stage Manual*," 2005, p. 4-18

Lovelock, J. E., "*Haemolysis of human red blood cells by freezing and thawing*," Biochimica et Biophysica Acta, 1953, 10, p. 414-426

Mazur, P., "*Kinetics of water loss from cells at subzero temperatures and the likelihood of intracellular freezing*," Journal of General Physiology, 1963, 47, p. 347-369

Mazur, P., "*Cryobiology: The freezing of biological systems*," Science, 1970, 168, p.939-949

Mazur, P., Leibo, S. P., Chu, E. H. Y., "*A two-factor hypothesis of freezing injury*," Experimental Cell Research, 1972, 71, p. 345-355

Mazur, P., "*The role of intracellular freezing in the death of cells cooled at supraoptimal rates*," Cryobiology, 1977, 14, p. 251-272

Mazur, P., "*Freezing of living systems: mechanisms and implications*," American Journal of Cell Physiology, 1984, 247(3), p. C125-C142

McGrath, J. J., Cravalho, E. G., Huggins, C. E., "*An experimental comparison of intracellular ice formation and freeze-thaw survival of HeLa S-3 cells*," Cryobiology, 1975, 12, p. 540-550

McGrath, J. J., "*Preservation of biological material by freezing and thawing*," Heat transfer in medicine and biology, A. Shitzer and R.C Eberhart (eds.), Plenum Press., New York, 1985

McGrath, J. J., "*Membrane transport properties*," In: McGrath, J. J., Diller, K. R (eds.), Low temperature biotechnology: Emerging applications and engineering contributions, 1988, BED – Vol. 10, HTD – Vol. 98, ASME Press, p. 273-330

Meyer, E. D., Sinclair, N. A., Nagy, B., "*Comparison of the survival and metabolic activity of psychophilic and mesophilic yeasts subjected to freeze-thaw stress*," Applied Microbiology, 1975, 29, p. 739-744

Molisch, H., "*Investigations on the freezing of plants*," Cryo-Letters, 1982, 3, p. 331-390

Müller-Thurgau, H., "*Concerning freezing and freezing death in plants*," 9, 1880, p. 133-189

Nag, K. K., and Street, H. E., "*Carrot embyo-genesis from frozen cultured cells*," Nature, 1973, 245, p. 270-272

Oegema, T. R., Deloria, L. B., Fedewa, M., Bischof, J. C., Lewis, J. L., "*A simple cryopreservation method for the maintenance of cell viability and mechanical integrity of cultured cartilage analog*," Cryobiology, 1999, 40, p. 370-375

Pawelec, G., Borowitz, A., Krammer, P. H., Wernet, P., "*Constitutive interleukin2 production by the JURKAT human leukemic T cell line*," European Journal of Immunology, 1982, 12(5), p. 387-392

Pringsheim, E. G., "*Julius Sachs: Founder of modern plant physiology*, *1832-1897*," Verlag Von Gustav Fischer, Jena, 1932

Raccach, M., Rottem, S., Razin, S., "*Survival of frozen mycoplasmas*," Applied Microbiology, 1975, 30, p. 167-171

Rebecca, S., "*Cells that save lives are a mother's legacy*," The New York Times, 2001

Salinas-Flores, L., Adams, S. L., Wharton, D. A., Downes, M. F., Lim, M. H., "*Survival of Pacific oyster, Crassostrea gigas, oocytes in relation to intracellular ice formation*," Cryobiology, 2008, 56, p. 28-35

Salinas-Flores, L., Adams, S. L., Lim, M. H., "*Determination of the membrane permeability characteristics of Pacific oyster, Crassostrea gigas, oocytes and development of optimized methods to add and remove ethylene glycol*," Cryobiology, 2008, 56, p. 43-52

Shabana, M., and McGrath, J. J., "*Cryomicroscope investigation and thermodynamic modeling of the freezing of unfertilized hamster ova*," Cryobiology, 1988, 25, p. 338-354

Schwartz, G. J., and Diller, K. R., "*Osmotic response of individual cells during freezing: II. Membrane permeability analysis*," Cryobiology, 1983, 20, p. 542-552

Simon, E. M., "*Freezing and storage in liquid nitrogen of axenically and monoxenically cultivated Tetrahymena pyriformis*," Cryobiology, 1972, 9, p. 75-81

Tervit, H. R., Adams, S. L., Roberts, R. D., McGowan, L. T., Pugh, P. A., Smith, J. F., Janke, A. R., "*Successful cryopreservation of Pacific Oyster(Crassostrea gigas) oocytes*," Cryobiology, 2005, 51(2), p. 142-151

Thirumala, S., Ferrer, M. S., Al-Jarrah, A., Eilts, B. E., Paccamonti, D. L., Devireddy, R. V., "*Cryopreservation of canine spermatozoa: theoretical prediction of optimal cooling rates in presence and absence of cryoprotective agents*," Cryobiology, 2003, 47(2), p. 109-124

Thirumala, S., "*Optimal rate of freezing biological systems*," MS thesis, 2004, p. 1-91

Thirumala, S., and Devireddy, R. V., "*A simplified procedure to determine the optimal rate of freezing biological system,*" Journal of Biomechanical Engineering, 2005, 127, p. 295-300

Thirumala, S., Gimble, J., Devireddy, R. V., "*Transport phenomena during freezing of adipose tissue derived adult stem cells*," Biotechnology and Bioengineering, 2005, 92, p. 372-383

Thirumala, S., Campbell, W. T., Vicknair, M. R., Tiersch, T. R., Devireddy, R. V., "*Freezing response and optimal cooling rates for cryopreserving sperm cells of striped bass, Morone Sancatilis*," Theriogenology, 2006, 66(4), p. 964-973

Thirumala, S., Forman, J. M., Monroe, W. T, Devireddy R.V, "*Freezing and post-thaw apoptotic behavior of cells in the presence of palmitoyl nanogold particles*," Nanotechnology, 2007, 18, p. 1-12

Thorpe, P. E., Knight, S. C., Farrant, J., "*Optimal conditions for the preservation of mouse lymph node cells in liquid nitrogen using cooling rate techniques*," Cryobiology, 1976. 13, p. 126-133.

Tiersch, T. R., Introduction. In: Tiersch, T. R., Maxik, P. M., (eds.), "*Cryopreservation in Aquatic Species*," Baton Rouge, LA: World Aquaculture Society, 2000, p. xix-xxvi

Toner, M., Cravalho, E.G., and Karel, M., "*Thermodynamics and kinetics of intracellular ice formation during freezing of biological cells*," Journal of Applied Physics, 1990. 67, p. 1582-1593

Toner, M., Tompkins, R. G., Cravalho, E. G., Yarmush, M. L., "*Transport phenomena during freezing of isolated hepatocytes*," American Institute of Chemical Engineers Journal, 1992, 38, p. 1512-1522

Toner, M., "*Nucleation of ice crystals inside biological cells*," Advances in low temperature biology, 1993, 2, p. 1-51

Unic Marketing Group Ltd (795 Main Street, Suite 303, Moncton, NB, EIC IE9), "*New Brunswick Oyster Aquaculture – Market Study*," 2003

Walsh, J.R., "*Modeling and design of algal cryopreservation protocols*," Ph.D. Dissertation, 2003, The University of Texas at Austin, Austin Texas

Wolkers, W., Balasubramanian, S., Ongstad, E., Zec, H., Bischof, J., "*Effects of freezing on membranes and proteins in LNCaP Prostate tumor cells*," Biochim Biophys Acta., 2007, 1768(3), p. 728-736

Zhang, T., Rawson, D. M., "*Permeability of the vitelline membrane of zebra-fish (Brachydanio rerio) embryos to methanol and propane-1, 2-diol*," Cryo-Letters, 1996, 17, p. 273-280

Vita

Tathagata Acharya was born in the eastern Indian city of Patna in March, 1981. He got his primary and secondary education from St. Michael's High School, Patna. He graduated from high school (B.D. Memorial Institute, Kolkata (Calcutta)) in 2000. In 2004, he graduated from University of Pune with a baccalaureate degree in production engineering, where he stood 4^{th} in order of merit among 287 students in the university. In 2004, he was recruited by Kirloskar Oil Engines Ltd., to work for their department of research and development, where he worked till July 2006. Finally, he went to graduate school in Louisiana State University on August, 2006. He is a candidate for the degree of Master of Science in Mechanical Engineering to be awarded at the commencement of December, 2008. After completing his master's degree he will be joining Foster Wheeler USA Corporation, at Houston, Texas, as a vessel engineer on January 5, 2009.